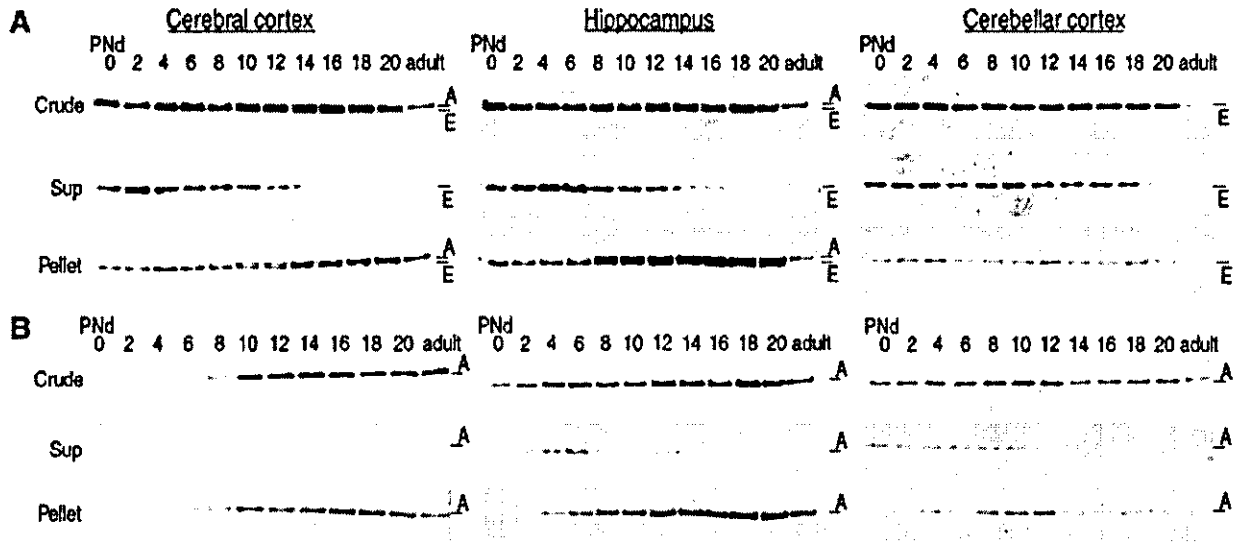

Fig. 2. Developmental changes in drebrin isoforms and subcellular distribution in rat brain as revealed by Western blotting. The supernatant and pellet fractions were obtained from the crude fraction of rat brain at various developmental stages from postnatal day (PNd) 0 to adult (postnatal week 15, PNw15) by centrifugation at 200,000 × *g*. Each fraction, equivalent to 0.23 mg of wet weight tissue, was analyzed in Western blot for the presence of drebrin A and drebrin E. **A:** The drebrin isoforms A and E are detected using the monoclonal antibody M2F6. **B:** The drebrin A-band was detected by using an antibody, DAS1, directed against the amino acid sequence unique to drebrin A (Shirao et al., 1994). Left column is cerebral cortex; middle column is hippocampus; and right column is cerebellar cortex. Details of the procedure appear under the Materials and Methods section.

RESULTS

Developmental change of drebrin isoform expression

We analyzed the developmental change of drebrin isoform expression in the cerebral cortex, hippocampus, and cerebellum. Western blot analysis showed that the expression level of drebrin E in the cortex was relatively constant during the first 2 weeks after birth, based on measurements of immunoreactivity of the lower band using the monoclonal antibody M2F6 (lower band in Crude of Fig. 2A, left column). Immunoreactivity of the lower band decreased gradually and was hardly detectable in adulthood. A similar developmental expression pattern of drebrin was observed in the hippocampus (Crude of Fig. 2A, middle column). In comparison, drebrin E decreased more slowly in the cerebellar cortex (Crude of Fig. 2A, right column) than in the cerebral cortex and or in the hippocampus.

The expression of drebrin A in the cerebral cortex, measured using M2F6 (upper band in Crude of Fig. 2A, left column) or using the drebrin A-specific antibody, DAS1 (Crude of Fig. 2B, left column), increased sharply at around PNd10. The expression of drebrin A also increased in the hippocampus at around the same age (Crude of Fig. 2B, middle column). In the cerebellar cortex, M2F6 barely detected drebrin A throughout development (Crude of Fig. 2A, right column). A faint band for drebrin A, recognized by DAS1, increased at around PNd10 but soon decreased and never showed such sharp increases as was seen for the cerebral cortex or the hippocampus (Crude of Fig. 2B, right column).

Disappearance of drebrin from the supernatant fraction in parallel with neuronal development

To assess the subcellular distribution of drebrin isoforms during postnatal development, homogenates, prepared in the presence of the mild nonionic detergent, NP-40, were fractionated into the supernatant and the pellet fractions by centrifugation. Drebrin E and drebrin A in homogenates of the cortex, the hippocampus, and the cerebellum were analyzed by Western blot. The supernatant was interpreted to be cytoplasmic or membranous, whereas the pellet was interpreted to be bound to organelles, possibly including F-actin (Fox, 1985; Crosbie et al., 1991).

Drebrin E. Before PNd12, drebrin E in cortex was detected in both the supernatant and pellet, using the monoclonal antibody M2F6. However, the protein level in the supernatant fraction decreased rapidly at around PNd14 and was no longer detectable by PNd20 (Sup of Fig. 2A, left column). On the other hand, the level of drebrin E in the pellet fraction was relatively constant until PNd20 (Pellet of Fig. 2A, left column). This developmental change in the subcellular distribution of cortical drebrin E was observed also for the hippocampus and the cerebellar cortex, although the change in the cerebellar cortex was not as sharp (middle and right columns of Fig. 2A).

Drebrin A. The emergence of drebrin A was detectable using the monoclonal antibody M2F6 (Fig. 2A). To investigate the appearance of drebrin A more directly, a polyclonal antibody, DAS1, that recognizes only drebrin A (and not drebrin E; Shirao et al., 1994) was used for the

Western blotting. A faint band of drebrin A in cortex was detected in both the supernatant and the pellet fractions at around PNd6. After PNd10, drebrin A in the cortex was barely detectable in the supernatant fraction but clearly was observed in the pellet fraction (Fig. 2B, left column). Drebrin A in the pellet increased in parallel with postnatal development.

The developmental change in the subcellular distribution of drebrin A in the hippocampus was similar to that in the cerebral cortex. Although drebrin A in the pellet fraction increased in parallel with development, drebrin A in the supernatant fraction disappeared after PNd14 (Fig. 2B, middle column). On the other hand, in the cerebellum, drebrin A in both the supernatant and the pellet fractions decreased after PNd14 (Fig. 2B, right column). Two regions—the cortex and the hippocampus—which showed particularly prominent developmental changes in the amount of drebrin A were chosen for further analysis of the cellular and subcellular distribution of drebrin A.

Light microscopy

Drebrin A immunoreactivity was analyzed throughout the cortical areas and hippocampus of PNd7 and adult tissue, using the newly generated antibody, DAS2 (Fig. 3). All three fixation conditions yielded similar patterns of immunolabeling and, thus, will not be described separately.

PNd7 cortex. PNd7 cortices exhibited a diffuse but darkened band that was midway between the pial surface and the white matter (Fig. 3). At a higher magnification (Fig. 4A1), it was evident that these bandings corresponded to delicate immunolabeling of perikaryal cytoplasm. Immunoreactive primary dendrites emanated horizontally from these perikarya within layer 5. Based on the size and the prominence of their apical dendrite that extended into layer 1 (white arrows in Fig. 4A1), these perikarya were identifiable as layer 5 pyramidal neurons. Layer 1 contained smaller puncta (<0.5 μm in diameter), immediately dorsal to the point where apical dendrites of the layer 5 pyramidal neurons formed tufts (white arrows in Fig. 4A1). The apical tufts and small puncta together formed an intense band within layer 1 (Fig. 3A). The most ventral, immunoreactive band within the cortex (SP in Fig. 3A) consisted of immunolabeled neurons residing immediately dorsal to the corpus callosum. These were multipolar, nonpyramidal neurons of the subplate (also referred to as layer 6b; Fig. 4A2). Some of the immunoreactive processes in this layer appeared long, varicose, and more intensely labeled than were the perikarya in the same tier (white arrows in Fig. 4A2).

Adult cortex. In place of the dark banding that corresponded to layer 5 of the PNd7 cortex, drebrin A immunoreactivity was most dense in layer 1 (Figs. 3A, 4C). At higher magnifications, it became evident that immunoreactivity consisted of uniformly sized puncta, less than 0.5 μm in diameter (Fig. 4B1–3). These puncta were distributed throughout the neuropil but were not detectably associated with the main trunks of dendrites (white arrows in Fig. 4B2,B3) or with neuronal perikarya (white asterisks in Fig. 4B3). Sections immunolabeled using the preadsorbed DAS2 showed complete elimination of the small puncta, whereas the diffuse labeling within the nucleus remained.

PNd7 and adult hippocampus. Labeling of the hippocampus resembled the pattern seen in the cortex. As seen for the PNd7 layer 5 pyramidal neurons, pyramidal neurons in the CA1–CA3 fields and the granule cells in the dentate gyrus exhibited prominent, continuous labeling within dendritic branches at PNd7 (Fig. 3B,C). Also, as seen for the adult cortex, the adult CA1 exhibited high density of immunolabeled puncta, and these puncta were not detectable over the primary dendrites' trunks or neuronal perikarya (Fig. 3D). The immunoreactive puncta were of markedly heightened density in the stratum lacunosum moleculare.

Immunolabeled puncta in stratum lucidum of the CA3 field also were fine, and these coalesced along the surface of major dendritic trunks of the CA3 pyramidal neurons (Fig. 3F). Puncta were even more intense in the stratum oriens of the CA3 field (Fig. 3F). In contrast to the adult cortex, adult pyramidal neurons in the CA3 field and granule cells in the dentate gyrus also retained the neonate-like form of labeling, i.e., continuous labeling within dendrites (Fig. 3E).

The puncta seen in adult tissue matched the sizes of spine heads, and the laminar distribution of the puncta matched the reported laminar distribution of excitatory synapses (Petralia and Wenthold, 1992; Megias et al., 2001; Levy and Aoki, 2002). These puncta were eliminated completely when the DAS2 antibody was preadsorbed. This observation indicated that the puncta reflected discrete, specific immunolabeling. We surmised that the differences seen between the two ages could reflect alteration in the subcellular distribution of drebrin A, as was indicated by the light microscopic and biochemical results, i.e., from the cytoplasm and plasma membrane of dendritic trunks and perikarya to spines. To determine whether drebrin A was localized to the cytoplasm of perikarya and dendritic trunks at PNd7 and became distributed more distally to spine heads in adulthood, electron microscopy was performed. Electron microscopy was also used to analyze the distribution of drebrin A in relation to the newly forming and well-established synaptic junctions within single PNd7 tissue.

Electron microscopy

For electron microscopic analyses, adult cortex and hippocampus were analyzed first, because it was easier to identify axons, dendritic shafts, and dendritic spines within adult tissue than in PNd7 tissue. Within the adult tissue, we aimed to establish whether drebrin A occurred pre- or postsynaptically or on both sides of synapses. The following morphological criteria were used to identify synapses as asymmetric: presence of vesicles, typically clustered into a group of 10 or more, near the synaptic cleft; thick coating along the intracellular surface of the other profile, recognized as the PSD. These were presumed to be excitatory, based on earlier studies that used immunoreactivity of synapses to AMPA and NMDA receptor subunits as indicators (Petralia and Wenthold, 1992; Aoki et al., 1994; Farb et al., 1995; Aoki, 1997; He et al., 1998). In the present study, we also verified that the presynaptic terminals of asymmetric synapses were consistently GABA-negative, based on PEG immunolabeling for GABA upon a subset of grids (Fig. 5A).

Twenty-three percent of the adult cortical synapses lacked PSDs. These will be referred to as symmetric and were presumed to be inhibitory or modulatory (Purpura and Pappas, 1972; Megias et al., 2001; Marty et al., 2002; Peters, 2002; Minelli et al., 2003). Immunolabeling for

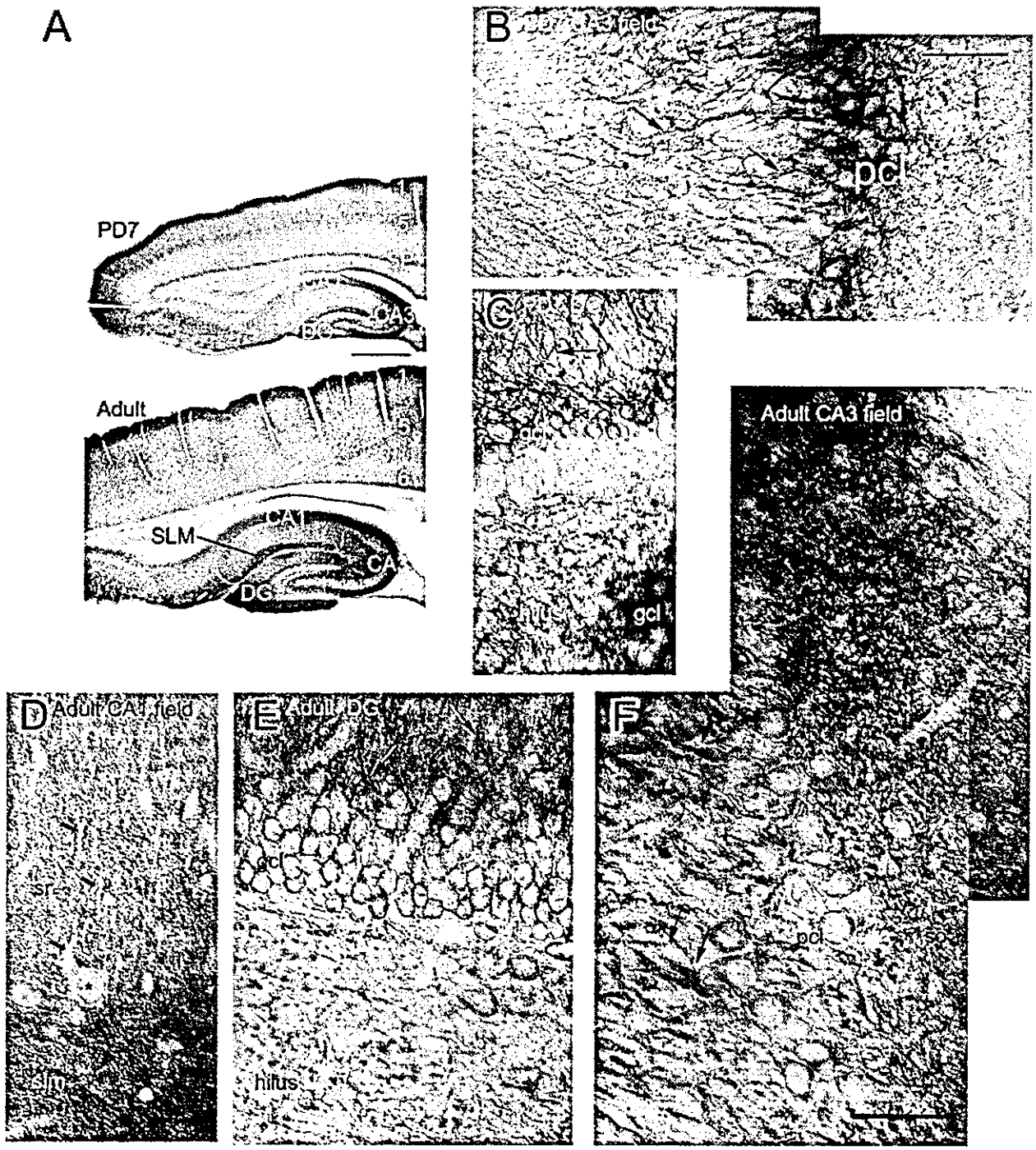

Fig. 3. Drebrin A immunoreactivity within postnatal day (PNd) 7 and adult cortex and the hippocampal formation. **A:** Sagittal sections show the overall distribution of drebrin A immunoreactivity, as revealed using the new drebrin A-specific antibody DAS2. At both ages, drebrin A immunoreactivity is particularly intense in the CA3 field of the hippocampus, the infrapyramidal leaf of the dentate gyrus (DG), and layer 1 of cortex. At PNd7 but not in adult, banding is also evident in the upper blade of the dentate gyrus as well as layers 5 and the subplate (SP) of cortex. In adulthood, but not at PD7, the stratum lacunosum moleculare (SLM) shows high concentration of immunoreactivity. **B,C:** Montages of light photomicrographs showing details of drebrin A immunoreactivity in the hippocampus of a PNd7 brain. **D–F:** Montages from an adult brain. At this magnification, it is evident that drebrin A immunoreactivity undergoes a laminar shift during development. At PNd7, immunoreactivity is intense in the perikaryal cytoplasm (labeled "pcl" for the pyramidal cell layer and "gcl" for the granule cell layer). Equivalent levels of immunoreactivity can be traced into the dendrites (arrows). In contrast, within the adult hippocampal formation, immunoreactivity is barely detectable within the cell bodies (asterisk), but is more intense within the synaptic layers. Immunolabeling is not contiguous, as seen in PNd7 brain but, instead, consists of high densities of puncta. D: Within the synaptic layers of the CA1 field (sr = stratum radiatum), the cytoplasm of apical dendrites' shafts appears unlabeled (arrows). Note the particularly intense labeling of puncta in the stratum lacunosum moleculare (slm). F: In stratum lucidum of the CA3 field, it is evident that these puncta aggregate along dendritic shafts (arrows). At both ages, immunoreactive puncta occur more dispersed in the hilus of the dentate gyrus. These dispersed puncta in the hilus are larger than the puncta coating dendrites. Most likely, these are cross-sectioned dendritic shafts. DG, dentate gyrus; gcl, granule cell layer; pcl, pyramidal cell layer; SLM, stratum lacunosum moleculare; so, stratum oriens; sr, stratum radiatum; sp, subplate. Scale bars = 1 mm in A, 50 μm in B,F (applies to B–F).

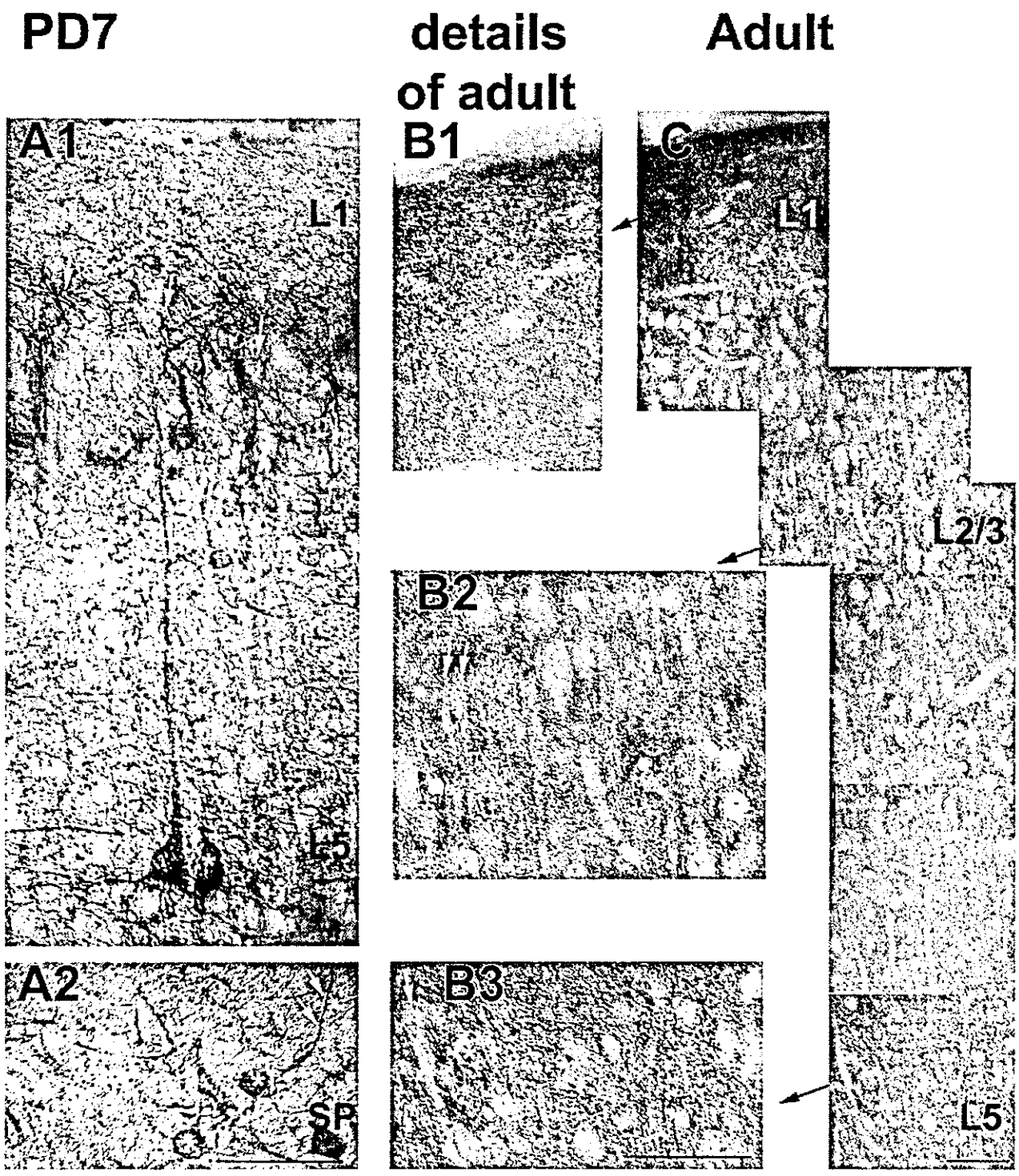

Fig. 4. Details of immunoreactivity in the neocortex at postnatal day (PNd, PD) 7 and in adulthood. **A1:** A montage showing drebrin A immunoreactivity in and surrounding a layer-5 pyramidal cell of PNd7 somatosensory cortex. The vertically oriented white arrows point to immunoreactivity within tufts of apical dendrites at the base of layer 1 (L1). Immunoreactivity continues along the apical dendrite of one cell that can be followed down to layer 5 (five angled, white arrows). The soma of this and the immediately neighboring cell (asterisk) show evenly distributed immunolabeling within the cytoplasm. **A2:** The subplate (SP, also referred to as layer 6b) of the same cortical tissue. Drebrin A immunolabeling is moderate within somata (asterisks) and more intense within dendrites (white arrows). **B1,B2,B3:** The middle column shows neuropil labeling of adult cortex, photographed and shown at the same magnification as that of the PNd7 tissue. In contrast to the PNd7 tissue, immunoreactivity is absent from the somata (asterisks in B3) but, instead, is distributed throughout the neuropil in the form of puncta. The white angled arrows point to examples of dendritic shafts, revealed by the absence of immunoreactivity.**C:** The right column shows a montage of the same adult neocortex, reduced in magnification to show the layers continuously. At this magnification, the unlabeled perikarya, embedded within the synaptic neuropil of the gray matter, are easily detectable from layers 2 through 5 (L1, L2/3, L5). All photomicrographs were obtained from sections immunolabeled using the newly generated drebrin A-specific antibody DAS2. Scale bars = 50 μm in A2 (applies to A1,A2), B3 (applies to B1–B3), C.

Fig. 5. Electron microscopic localization of drebrin A in adult cortex and hippocampus. A–D: Horseradish peroxidase–diaminobenzidine was used as the label to visualize drebrin A sites stratum oriens of the CA1 field of hippocampus (A,B) and in layer 6 of adult somatosensory cortex (C,D). All photomicrographs were obtained from sections that were immunolabeled using the new drebrin A-specific antibody DAS2. **A:** In A, only, immunoreactivity to γ-aminobutyric acid (GABA) is also shown by the postembedding immunogold labeling procedure (PEG) and also shows an absence of drebrin A labeling along somatic, symmetric synapses (filled arrowheads). These are inhibitory axosomatic synapses, as evidenced by the immunoreactivity of the axon terminal to GABA (GABA-T). In contrast, an asymmetric, axospinous synaptic junction immediately above the GABA-Ts is drebrin A immunoreactive on the postsynaptic side (arrow). Immunoreactivity appears diffusely within the spine cytoplasm (Drebrin + Sp). Based on the thickness of the postsynaptic density and the absence of GABA in the presynaptic terminal (nonGABA-T1), this synapse is likely to be glutamatergic and excitatory. Another spine to the right is unlabeled for drebrin A (open arrowhead), even though it is postsynaptic to a non-GABAergic terminal (nonGABAergic T2, probably glutamatergic). **B:** An adjacent ultrathin section from the hippocampus is shown. Drebrin A immunoreactivity is more intense, because this tissue has not undergone the osmium-extraction step required for the PEG shown in A. B also shows an unlabeled symmetric synapse (filled arrowhead, at the dendritic shaft, DS), an unlabeled asymmetric synapse (open arrowhead, on a spine), and many more drebrin A-immunolabeled asymmetric synapses on spine heads (arrows). BVL, blood vessel lumen. **C:** Two asymmetric synapses associated with a single axon terminal, one of which is immunolabeled (right, arrow) and the other of which is unlabeled (left, arrowhead). **D:** Heterogeneous labeling among spine heads, all located at the resin-tissue interface and, therefore, expected to have received optimal exposure to immunoreagents. Arrows point to immunolabeled spines' postsynaptic densities, whereas the arrowheads point to unlabeled asymmetric synapses. Scale bar = 500 nm in B (applies to A–C); 565 nm for D.

TABLE 1. Ultrastructural Characteristics of Synapses in Relation to Drebrin A: Adult Cortex (190 encountered synapses)

Asymmetric 147				Symmetric 43			
Labeled 111		Unlabeled 36		Labeled 3		Unlabeled 40	
Spinous 106	On shaft 5	Spinous 29	On shaft 7	Spinous 0	On shaft 3	Spinous 0	On shaft 40

TABLE 2. Ultrastructural Characteristics of Synapses in Relation to Drebrin A: Adult Hippocampus (179 encountered synapses)

Asymmetric 150				Symmetric 29			
Labeled 102		Unlabeled 48		Labeled 0		Unlabeled 29	
Spinous 99	On shaft 3	Spinous 44	On shaft 4	Spinous 0	On shaft 0	Spinous 0	On shaft 29

GABA by the PEG procedure upon a subset of grids verified that axon terminals forming symmetric synapses were GABAergic (Fig. 5A).

All three fixation conditions used for the study yielded excellent preservation of the ultrastructure and antigenicity, thereby allowing for sampling of synapses at surface-most regions of tissue, where penetration by immunoreagents would be the greatest. The proportion of encountered synapses with detectable levels of labeling did not differ greatly across the layers. Thus, the immunolabeling features described below apply to all layers.

Adult tissue, labeled using HRP-DAB: Asymmetric synapses are drebrin A-positive on the postsynaptic side. Twenty nonoverlapping fields along the tissue-resin interface were sampled from the adult cortical tissue, covering 245 μm^2 of the neuropil, mostly from the infragranular layers. 77% of the encountered synaptic profiles (147 of 190) were identifiable as asymmetric (Table 1) and of these, 76% (111 of 147) were detectably immunolabeled for drebrin A (Table 1). Drebrin A immunoreactivity was never on the presynaptic side. An analogous survey was performed for the adult hippocampus, using 14 non-overlapping fields, spanning 171.5 μm^2 of the neuropil, mostly from the infrapyramidal leaf of the dentate gyrus. A total of 179 synapses were encountered and of these 84% (150 of 179) were asymmetric (Table 2) and of these, 68% (102 of 150) were immunolabeled for drebrin A (Table 2). Again, immunoreactivity was strictly on the postsynaptic side.

Unlabeled asymmetric junctions occurred immediately adjacent to immunolabeled asymmetric synapses (Fig. 5). A striking example of the juxtaposition of immunolabeled and unlabeled synapses is shown in Figure 5C. Here, the two synapses are immediately adjacent to one another and receiving inputs from a single presynaptic terminal. Juxtaposition of labeled and unlabeled asymmetric synapses occurred even along the extreme edges of tissue (Fig. 5D), where large portions of the dendritic shafts were visibly cut open by the Vibratome knife. Such observations indicated that lack of immunoreactivity to drebrin A cannot be explained entirely by failure of immunoreagents to penetrate tissue. Rather, these observations indicated that asymmetric synapses of adult cortices and hippocampi vary in drebrin A content.

Analysis of the tissue immunolabeled using the preadsorbed DAS2 antibody indicated further that the labeling of asymmetric synapses was specific: the percentage of asymmetric synapses that were detectably immunolabeled was reduced from approximately 80% down to 7%, accompanied by a markedly reduced intensity of immunolabeling within the individual spines.

Large subset of the drebrin A-immunoreactive asymmetric synapses is axospinous. The great majority of immunolabeled synaptic junctions with thick PSDs in the cortex (95%, 106 of 111) and hippocampus (97%, 99 of 102) were axospinous (Fig. 5A; Tables 1, 2). On the other hand, asymmetric junctions on dendritic shafts of cortex also were drebrin A immunoreactive (5 of 12 in cortex, 3 of 7 in hippocampus; Tables 1, 2), indicating that spinous location was not a strict requirement for the presence of drebrin A. Conversely, more than half of the asymmetric synaptic junctions on shafts were unlabeled, as opposed to approximately one third to one-quarter of the axospinous asymmetric synaptic junctions that were unlabeled, indicating that drebrin A is preferentially clustered within spines.

Symmetric synapses have low amounts or no drebrin A. All of the symmetric synapses were on dendritic shafts and almost all of these were unlabeled for drebrin A (40 of 43 in cortex; 29 of 29 in hippocampus; black arrowheads in Fig. 5A). The three immunolabeled synapses on shafts that appeared symmetric may actually have been asymmetric synapses that were not sectioned at a favorable plane to reveal the presence of PSDs.

Neonatal tissue, labeled using HRP-DAB: Drebrin A occurs in dendrites, not axonal growth cones. Within neonatal tissue, labeling was apparent along the intracellular surface of plasma membranes. Considering the diffuse nature of HRP-DAB label in general, the immunoreactivity was surprisingly discrete, occurring as small patches that were immediately opposed to sites contacted by axons. These processes exhibiting drebrin-A immunoreactive patches were identifiable as dendrites, based on the smooth but irregular contour, large diameter, absence of vesicles, and occasional abutting with profiles identifiable as axonal. Not all dendrites exhibited clear arrays of microtubules (compare Fig. 6B,C, which shows no microtubules, with Fig. 6D, which shows microtubule arrays clearly). Axons, in turn, were identified based on the presence of a few vesicles. Typically, these vesicles were gathered at sites removed from the junctional membrane (Fig. 6A, synapse 2 in Fig. 6D, Fig. 6E). Only 1 of the 149 encountered synapses exhibited drebrin A immunoreactivity in a profile that was judged to be possibly axonal.

Drebrin A appearance precedes synapse formation. Unlike the adult tissue, drebrin-A immunoreactivity was present in profiles lacking any features identifiable as synaptic (Fig. 6B). Where spine-like protrusions could be detected, these appeared incompletely formed, in that the neck was still nearly as wide as the spine head (Fig 6A, right, and synapse 1 in Fig. 6D). In addition, those that appeared to be junctional were still immature, because the

Fig. 6. Ultrastructural localization of drebrin A in postnatal day (PNd) 7 cortex. Horseradish peroxidase–diaminobenzidine was used to detect the presence of drebrin A. **A:** A large-caliber axon that is largely devoid of vesicles, yet synaptically associated with two dendritic processes. Of the two small clusters of vesicles, only one is at a synapse. The synapse showing a slight indentation of the plasma membrane, perhaps an early sign of spine neck formation, lacks vesicles presynaptically. Both synapses show accumulation of drebrin A immunoreactivity along the postsynaptic membrane (arrows). **B:** A dendrite lacking morphologically identifiable synapses. Drebrin A immunoreactivity has accumulated along small protrusions (asterisks). **C:** A well-established spine head forming a synapse with an axon. The axon contains a moderate number of vesicles that are clustered at the synaptic junction, and the postsynaptic membrane (arrow) is slightly immunoreactive. Drebrin A immunoreactivity is more intense along the nonsynaptic portions of the plasma membrane. The nonsynaptic portions of the dendrite contain no detectable microtubules and also exhibit plasma membranes with irregular contours. **D:** A dendrite containing well-defined microtubules. Drebrin A immunoreactivity is evident along a slight protruding portion of the shaft (synapse 1) and along a spine with narrow neck (synapse 2) but whose presumably "presynaptic" profile shows no vesicle clustering near the juxtaposed portion of membrane. Drebrin A immunoreactivity is also associated with a dendritic shaft forming an asymmetric synapse (synapse 3) opposite of another protuberance (asterisk) and another dendritic protuberance (synapse 4) whose presynaptic element shows adult-like vesicle clustering. **E:** A dendrite bearing a spine that stains strongly for drebrin A. The neurite with which this immunoreactive spine is associated shows only a few vesicles, scattered widely and away from the juxtaposed portion of the plasma membrane. In contrast, the other presynaptic element associated with an unlabeled spine (arrowhead) of the same dendrite contains a large cluster of vesicles. Scale bar = 500 nm in E (applies to B–E); 650 nm for A.

TABLE 3. Ultrastructural Characteristics of Synapses in Relation to Drebin A: PNd7 Cortex (149 Encountered Synapses)

Asymmetric 93				Symmetric 56			
Labeled 40		Unlabeled 53		Labeled 18		Unlabeled 38	
Mature 2	Immature 38	Mature 4	Immature 49	Mature 0	Immature 18	Mature 0	Immature 38

PNd, postnatal day.

PSDs were often absent (left arrow in Fig. 6A, Fig. 6C) and the putatively presynaptic profile contained either no vesicle near the junctional membrane (Fig. 6A,D), only a few vesicles (right synapse with straight arrow in Fig. 6A, synapse 1 of Fig. 6D, Fig. 6E), or many more vesicles that were removed from the junctional membrane (synapse 2 in Fig. 6D). We noted that some dendritic profiles showed more intense drebrin A immunoreactivity in the nonjunctional portions than in the synaptic portions (e.g., Fig. 6C).

Majority of asymmetric synapses are immature and unlabeled for drebrin A. Quantitative analysis was performed upon neonatal cortex, categorizing synapses either as newly formed, immature, and presumed to be synaptic, or as mature. The number of vesicles, detectability of PSDs and narrowness of spine necks were used as criteria to distinguish between the two categories. Those intercellular contact sites lacking both the PSDs and vesicles were categorized as nonsynaptic. Twenty-six nonoverlapping fields were surveyed from which were found 149 synaptic profiles (labeled and unlabeled, asymmetric and symmetric) and 31 nonsynaptic immunolabeled profiles. Ninety-six percent of these profiles appeared immature, using the above criteria. Unlike the adult tissue, in which the majority of synapses were immunolabeled (114 of 190), only a minority (58 of 149) of the synaptic junctions encountered in PNd7 cortex were drebrin A immunoreactive (Labeled, symmetric + asymmetric; Table 3). This difference across the ages was statistically significant (58 ± 4% for adults, 31 ± 4% for PNd7 tissue; $P < 0.0005$, two-tailed unpaired t test). Among the synapses identifiable as asymmetric, the majority of those in the PNd7 cortex (53 of 93) were also unlabeled, as opposed to the adult cortex, for which only 36 of the 147 asymmetric synapses were unlabeled (Table 3). This difference across the ages was statistically significant (59 ± 8% for PNd7; 23 ± 5% for adult; $P < 0.005$, two-tailed unpaired t test).

Larger proportion of the presumptive immature symmetric synapses is immunolabeled for drebrin A. Another notable departure from adult tissue was the prevalence of drebrin A at symmetric junctions. Thirty-two percent (18 of 56) of the presumptive immature symmetric synapses in PNd7 cortex were immunolabeled (Table 3). Compared with the adult tissue, many more of the neonatal synapses were classified as symmetric, due to the absence of the PSDs (38% for PNd7-tissue, 23% for adult tissue; Table 3). Most likely, many of these were glutamatergic synapses in which the PSD had not yet assumed their mature thick form and in which the spine necks had not yet narrowed (Aoki et al., 1994; Aoki, 1997).

Two PEG immunolabeling results supported the above presumption that neonatal synapses exhibiting drebrin A are excitatory. One was that the axons identifiable to be presynaptic to the drebrin A-positive dendritic membrane were almost always GABA-negative (more than 90% of the drebrin A-positive synapses encountered, an example shown in Fig. 7), with some of the exceptions consisting of dendrites receiving convergent inputs from multiple axons that included GABA-positive ones. The second was that dendritic membranes, revealed to be drebrin A-positive by the SIG label (detailed below), also were immunopositive for the NR2B subunit of NMDA receptors (an example shown in Fig. 8).

Adult tissue, immunolabeled for drebrin A using SIG, exhibit dendritic localizations. Another set of tissue was immunolabeled using SIG, so as to be able to analyze the distribution of drebrin A within postsynaptic profiles. Although light microscopy indicated only low amounts of drebrin A in perikarya and dendritic trunks, electron microscopy revealed discrete labeling along the intracellular surface of perikarya (data not shown). These immunoreactive sites of perikaryal plasma membranes were not synaptic. The immunoreactive patches of the membrane typically occurred adjacent to arrays of endoplasmic reticulum.

Synaptic labeling with SIG was exclusively postsynaptic and at asymmetric synapses. The proportion of synapses labeled (30 of 51 or 59%) was lower than that seen using HRP-DAB (111 of 147 or 76%), indicating that many more synapses may have expressed drebrin A but at amounts too low to be detectable by the less-sensitive SIG procedure. Nevertheless, the SIG-labeled tissue could be used to reveal more precise information regarding the intracellular distribution of drebrin A. Drebrin A was detected immediately adjacent to PSDs (Fig. 9B). However, more often, SIG particles within dendrites occurred along membranous portions removed from PSDs (Fig. 9A), indicating that a larger pool of drebrin A exists at nonjunctional sites.

Neonatal tissue, labeled using SIG, shows enrichment of drebrin A at presumptive immature synapses. Neonatal tissues were also subjected to drebrin-A immunolabeling using SIG. As expected, the proportion of synaptic profiles labeled by the SIG label was less, compared with the HRP-DAB labeling. Nevertheless, the SIG labeling resembled the DAB labeling's developmental pattern, in that the proportion of synapses labeled was less at PNd7 (9 of 31 or 29%) than in adulthood (59%).

The SIG procedure revealed an additional feature regarding drebrin A, namely that the presumptive immature synapses are more frequently labeled than are the synapses with relatively more established morphological characteristics. Some of the immunoreactive sites showed no intercellular specializations, whereas other immunoreactive sites were synapses with distinctively immature features (arrowheads in Fig. 10). In contrast, mature synapses with clearly identifiable PSDs in the immediate vicinity were frequently unlabeled (open arrows in Fig. 10). Over the scanned area, only 1 of the 24 mature synapses encountered within PNd7 tissue was immunolabeled by SIG, in contrast to 9 of the 21 presumptive immature synapses encountered that were immunolabeled. These observations indicated that the amount of

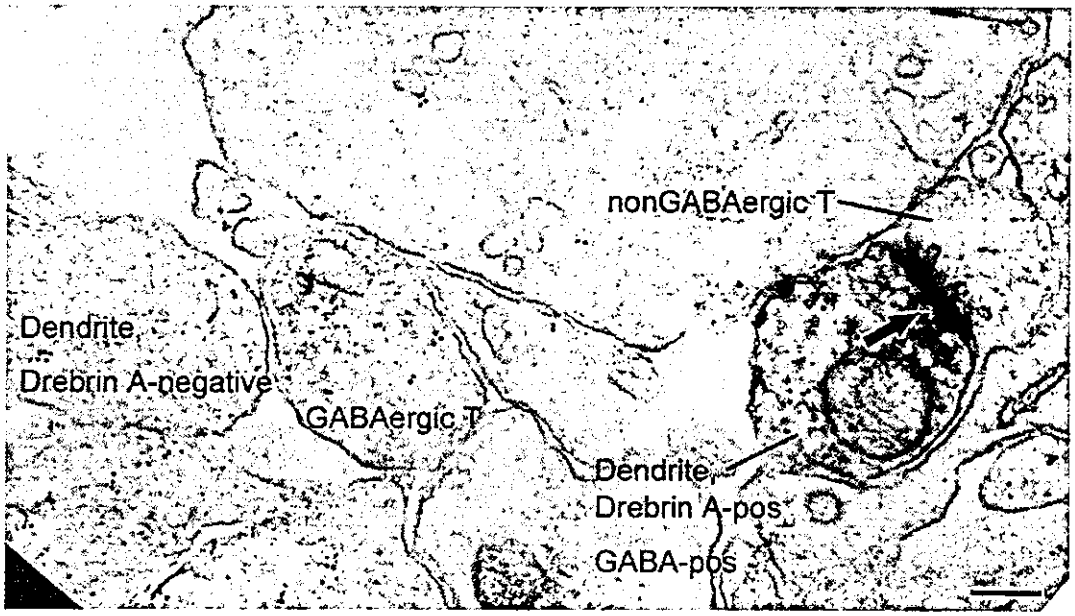

Fig. 7. Drebrin A is postsynaptic to γ-aminobutyric acid (GABA) -negative terminals of postnatal day (PNd) 7 tissue. At PNd7, dendrites rarely exhibit axospinous asymmetric synapses, thereby making the distinction between excitatory and inhibitory synapses more difficult than for adult tissue. The section shown here was dually labeled for drebrin A (by horseradish peroxidase–diaminobenzidine [HRP-DAB]) and for the inhibitory neurotransmitter, GABA by the postembedding gold immunolabeling procedure (PEG). The 10-nm colloidal particles reflect GABA immunoreactivity. GABA immunoreactivity is detectable in one profile that appears to be an axon terminal (GABAergic T), based on the presence of a few vesicles. This profile is juxtaposed to a drebrin A-negative profile that is likely to be a dendrite. In contrast, the dendrite to the right is HRP-DAB–labeled for drebrin A (Drebrin A-pos) and is also immunoreactive for GABA (GABA-pos). However, its presynaptic terminal is completely devoid of 10-nm colloidal gold particles, indicating that is it non-GABAergic (nonGABAergic T). The arrow points to the postsynaptic membrane over which drebrin A accumulates. Scale bar = 200 nm.

drebrin A expressed at single synapses varied, with mature synapses exhibiting relatively less than the newly forming ones. Examples were seen where two axons converged upon a single postsynaptic profile, with each axon abutting a distinct spine head (Fig. 10B). Here, too, drebrin A immunoreactivity was more robust within the less mature spine head, so identified by the absence of PSD and absence of vesicle clusters within the abutting portion of the axon.

Although the SIG labeling for drebrin A was not strictly along the postsynaptic membrane (small arrows in Fig. 10), it appeared to be biased toward the inner surface of the dendritic plasma membrane, rather than being distributed evenly in the cytosol. Quantitative analysis of SIG particle positions showed that the above impressions regarding the membranous bias of labeling were valid. The 331 SIG particles encountered within the 46 nonoverlapping surveyed fields were collected from two PNd7 and two adult brains; 20% of the SIG particles occurred directly on the membrane, and 45% remained within 50 nm from the plasma membrane. This distance corresponded to the 0 to 10% distance from the plasma membrane, relative to the diameter of the profiles (Fig. 11). This proximity of drebrin A sites to the membrane was relatively more prominent for the PNd7 tissue. Specifically, 56% of the SIG particles for one PNd7 tissue occurred within the 10% distance from the plasma membrane, and the corresponding value for the other PNd7 tissue was 64%. Both of these values were greater than the value obtained for the two adult tissue—40% and 41% (Fig. 11). However, data from more animals will need to be collected before we can be certain about the age-dependent differences.

Western blotting reveals developmental loss of drebrin A in the supernatant. The electron microscopic observation showing association of drebrin A with the intracellular surface of the plasma membrane prompted us to further quantify the subcellular distribution of drebrin. To this end, Western blotting was performed to obtain quantitative measures of drebrin in the supernatant (mostly free cytosolic, but also including drebrin associated with the membrane) and in the pellet (mostly associated with F-actin and microsomes) fractions (Fox, 1985; Crosbie et al., 1991). Based on the developmental data obtained from Western blotting (Fig. 2), PNd8 was taken as the representative ages of the neonatal stage (where a large portion of the drebrin is still in the E-isoform), whereas PNd16 was taken as the representative, youngest adult-like stage, in which the A-isoform dominates.

Quantitative analysis of drebrin content in the PNd8 and PNd16 cortices was performed by measuring the intensity of Western blots, using the M2F6 monoclonal antibody that could recognize both the E and A isoforms (Fig. 12). In agreement with the decline of both the A and E isoforms of drebrin in the supernatant during development, the total drebrin intensity (drebrin A + drebrin E) in the supernatant fraction at PNd16 significantly decreased to 17.9 % of that at PNd8 ($P < 0.001$). In comparison, there was no significant difference in the actin intensity in the supernatant fraction between PNd8 and

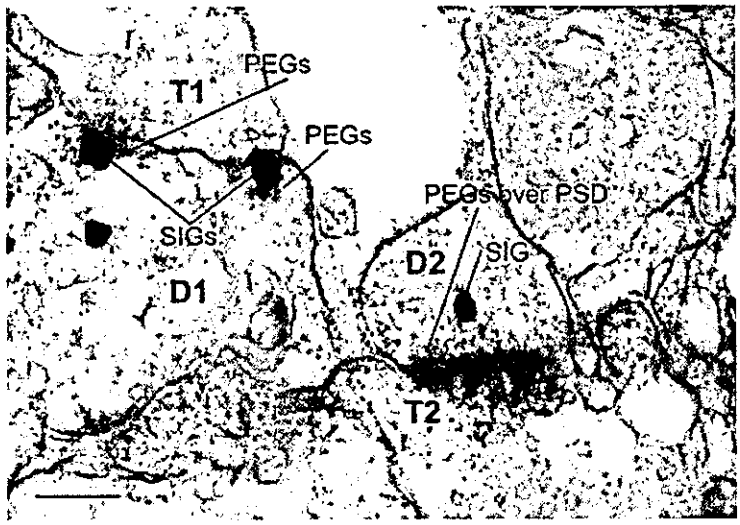

Fig. 8. Coexistence of drebrin A with the NR2B subunit of *N*-methyl-D-aspartate receptors at the postsynaptic membrane of a postnatal day (PNd) 7 dendrite. D1 to the left exhibits silver-intensified colloidal gold particles (SIG), reflecting immunoreactivity for drebrin A. Two of the SIG particles occur along the intracellular, postsynaptic membrane surface. Immediately adjacent to each of the SIG particles, two to four postembedding gold immunolabeling procedure (PEG) particles occur, reflecting the presence of low levels of NR2B subunits. The presynaptic terminal T1 contains only a few vesicles. In contrast, the terminal, T2, forming the adjacent synapse contains many vesicles, and the postsynaptic membrane of D2 exhibits a thick postsynaptic density (PSD). At least 12 PEG particles occur over the postsynaptic density, indicating the prevalence of NR2B subunits. This postsynaptic membrane does not show detectable levels of drebrin A. Instead, drebrin A immunoreactivity is slightly removed from the postsynaptic membrane. Scale bar = 200 nm.

PNd16. Also, in the crude homogenate or the pellet fraction, drebrin intensity did not change significantly between PNd8 and PNd16.

Based on previously published results, we surmised that the pellet fraction prepared after centrifugation at 200,000 × *g* represented the association of drebrin with F-actin (Ishikawa et al., 1994). Earlier studies had established that high salt could extract actin binding proteins from F-actin pellets (Glenney et al., 1982; Yamashiro-Matsumura and Matsumura, 1985). When this same procedure was used on our pellet fractions, a large portion of drebrin A was extracted from the pellet and entered the supernatant fraction (Fig 13). This outcome indicated that a large portion of drebrin A in the pellet was bound to the cytoskeleton and most likely to F-actin and microsomes and not to the plasma membrane.

DISCUSSION

The present study revealed a clear-cut segregation of drebrin A to postsynaptic sides of asymmetric synapses within mature cortex and hippocampus. During the phase of active synaptogenesis, drebrin A was present at the submembranous zone of dendritic plasma membranes before the formation of PSDs or spine heads, and also before the aggregation of vesicles presynaptically. This observation is consistent with results from our previous in vitro study, indicating that clustering of drebrin A precedes the formation of spines (Takahashi et al., 2003). Contrary to the presumptions we held before this ultrastructural study, our new observations indicate that drebrin E, *together with drebrin A*, are involved in the initial formation of protospines, rather than the involvement of drebrin E, alone. Moreover, the present ultrastructural study was able to verify that drebrin A occurs at membranous sites that were positively identifiable as synaptic, based on the emergence of a few vesicles, PSDs, and/or aggregation of glutamate receptor subunits there. The biochemical results indicate that the phase of synaptogenesis is paralleled by the increasing association of drebrin A with the pellet fraction containing actin. Below, we discuss the possibility that drebrin A may be involved in organizing the dendritic pool of actin for the formation of at least some of the spines and axospinous excitatory synapses.

Drebrin A is postsynaptic for excitatory synapses

The segregation of drebrin A to the postsynaptic side was clearer than it was for any of our previous observations of synaptic proteins, including the glutamatergic receptors (Aoki et al., 1994; Farb et al., 1995) and PSD-95 (Aoki et al., 2001). This was so, even though the immunolabeling for glutamatergic receptor subunits and PSD-95 faced similar technical limitations. We also noted absence of drebrin A at almost all of the mature symmetric synapses. Symmetric synapses are sites for inhibitory inputs, indicated by the clustering of $GABA_A$ receptor subunits, proteins such as gephyrin for the anchoring of these subunits and contacts formed by GABAergic axon terminals (reviewed by Fritschy and Brunig, 2003). Symmetric synapses also are associated with axons releasing neuromodulators, such as the monoamines and acetylcholine (Descarries, 1991).The segregation of labeling between symmetric and asymmetric synapses indicates that drebrin A is involved in the formation of at least some of the excitatory synapses but not of the GABAergic or purely modulatory synapses. Whether or not another organizer of F-actin occurs at GABAergic synapses remains unknown.

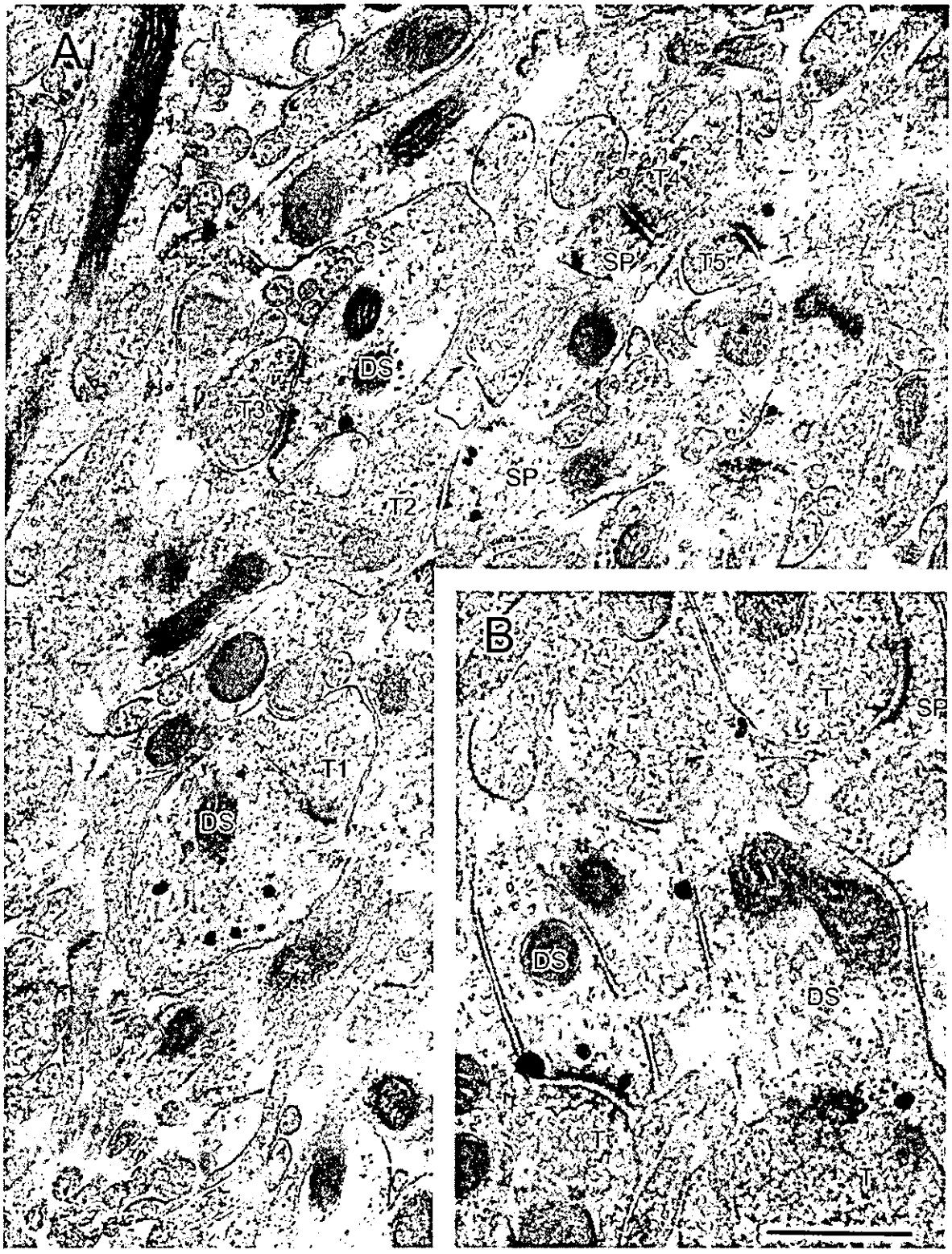

Fig. 9. Drebrin A in the synaptic neuropil of the molecular layer of the adult infrapyramidal dentate gyrus. Silver-intensified colloidal gold particles (SIG) were used to detect drebrin A. **A:** Five synapses, all asymmetric and associated with immunoreactivity to drebrin A on the postsynaptic side, only. The postsynaptic side is indicated as DS for dendritic shafts or as SP for spines, whereas the presynaptic profiles are indicated as T for terminal. At synapses formed with terminals T1, T2 and T3, the SIG particles occur along nonsynaptic portions of the plasma membrane and at the periphery of the postsynaptic density (PSD). At these synapses and all others, SIG particles occur in the cytoplasm as well. **B:** Three more synapses, two of which exhibit SIG particles discretely along the postsynaptic membrane. Additional SIG particles occur at nonjunctional sites. Scale bar = 666 nm in B; 500 nm for A.

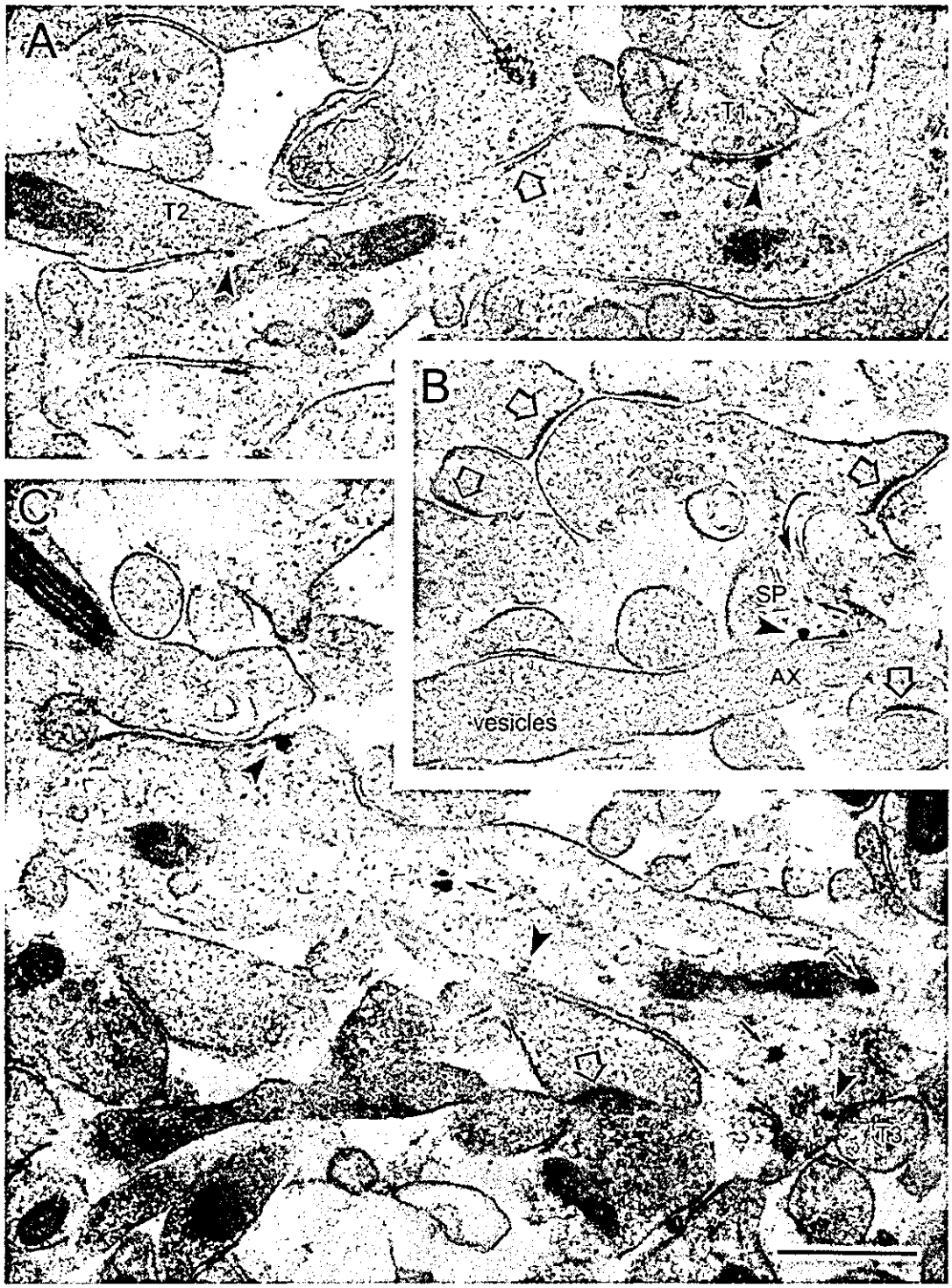

Fig. 10. Drebrin A in the molecular layer of postnatal day (PNd) 7 infrapyramidal dentate gyrus. Silver-intensified colloidal gold particles (SIG) were used as the label to detect the presence of drebrin A. **A:** Selective labeling along junctional portions of the plasma membrane. The arrowhead to the right shows SIG particles associated with a morphologically identifiable synapse (T1 marks the presynaptic terminal), whereas the SIG particle to the left shows no association with postsynaptic densities (PSDs). The immediately adjacent profile, T2, appears to be an axon terminal, indicating that this site is an immature synapse. The open arrow in the middle (and in other panels) points to a well-differentiated synapse lacking SIG particles. **B:** Three SIG particles occurring within a spine head (SP) lacking a PSD (arrowhead points to membranous SIG; small arrow to a cytoplasmic SIG). The immediately adjacent profile is an axon (Ax), as is evident by the cluster of vesicles in the same profile, toward the left. The same filopodia branches (curved arrow) from a more well-established but unlabeled spine with PSD (open arrows). **C:** A dendrite with irregular contours, no apparent microtubules, and containing six clusters of SIG particles. SIG occurs discretely along the plasma membrane forming a protuberance (arrowhead to the left) and contacting an axon. The arrowhead in the center points to an SIG particle along the plasma membrane that lacks apparent association with any axon. The arrowhead to the right points to the SIG particle associated with a portion of the plasma membrane beginning to form a PSD adjacent to an axon terminal, T. Arrows point to SIG particles in the cytoplasm, away from the plasma membrane. Scale bar = 500 nm in C (applies to A–C).

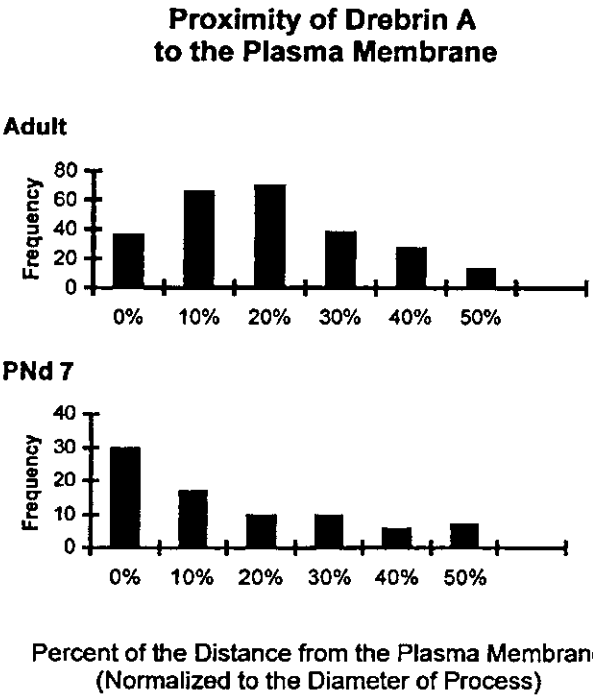

Fig. 11. Histograms showing the distribution of silver-intensified colloidal gold (SIG) particles in relation to the plasma membrane. The percentage values on the x-axis depict distances from the plasma membrane, normalized to the diameter of the profile in which the SIG particles are found. The y-axis depicts frequency of encounters at these varying distances from the membrane. Zero percent denotes SIG occurring at the plasma membrane. The encountered SIG particles were tallied from two postnatal day 7 and two adult hippocampal tissues.

Because GABAergic synapses occur at nonspinous portions of the plasma membrane, these synapses may not require F-actin binding proteins. Alternatively, a counterpart to an F-actin binding protein like drebrin may still be required at GABAergic synapses for the sake of receptor clustering and anchoring.

It has been shown previously that asymmetric synapses increase progressively in the neuropil during early postnatal development and that the spines emerge from stubby protospines along dendritic shafts after dendritic filopodia have disappeared (Vaughn, 1989; Harris, 1999; Jontes et al., 2000). Based on these observations, we surmise that PSDs convert from thin to thick during ontogeny, thereby converting synapses with symmetric appearances along protospines into those with asymmetric appearances at the spine heads. Our past (Aoki et al., 1994; Aoki, 1997) and present dual PEG immunocytochemical localization of glutamatergic receptor subunits corroborate this finding, because these receptors are found on synapses with very thin PSDs early on, and at progressively thicker PSDs in later weeks and in adulthood. The association of drebrin A with symmetric synapses at PNd7 and with asymmetric synapses in adulthood is likely to reflect drebrin A's association with newly formed glutamatergic synapses and of its persistence there during varying phases of maturation, rather than the switching of drebrin A from inhibitory to excitatory synapses during development. In support of this idea, drebrin A immunoreactivity was absent from symmetric synapses that had begun to acquire some of the morphological characteristics of mature GABAergic synapses (e.g., large cluster of vesicles that are associated along the presynaptic membrane; clearly defined microtubules within the postsynaptic dendrite, GABA immunoreactivity within the terminal). Drebrin A may be useful for identifying immature excitatory synapses before they acquire the more obvious morphological features. Studies are under way to determine whether the arrival of drebrin A to the dendritic membrane precedes arrival of NMDA receptor subunits or is linked to NMDA receptor recruitment.

Drebrin A arrives at dendritic membranes before synaptogenesis

By using both SIG and DAB as immunolabels for electron microscopy, we show that drebrin A appears at the earliest phase of synaptogenesis. Although neither label can be used to reveal the absolute values of drebrin A concentrations at junctions, the SIG label could be used to assess the relative concentration of antigens in the proximity of synaptic junctions. Our observations of tissue immunolabeled using HRP-DAB and SIG as the label indicate that the *proportion* of synaptic junctions lacking drebrin A immunoreactivity is greater at PNd7 than in adulthood. It has been reported that the turn-over rate of spines is higher in neonatal brain than in adult brain (Lendvai et al., 2000). It may be that drebrin A plays a role not only at the beginning of synaptogenesis and spinogenesis but also in the maintenance of spines. Once a spine loses drebrin A, that spine may be cleared from the neuropil more rapidly. If so, then the higher turnover rate of spines neonatally may be a consequence of a larger proportion of spines having lost drebrin A. Further experiments are needed to link physiological characteristics of spines to the presence of drebrin A and of the cause–effect relationship between spine turnover and drebrin A content.

Possible role of Drebrin A in neonatal cortex and hippocampus

In this study, we show that the rapid increase of drebrin A is paralleled by the disappearance of drebrin from the supernatant fraction at PNd8. Because we prepared crude homogenates in the presence of a mild detergent, NP-40, we expect the supernatant fraction to contain proteins that are free in the cytosol or solubilized from the membrane. Although G-actin (actin monomers) occurs in high amounts in the supernatant, we know that drebrin does not associate with actin monomers (Ishikawa et al., 1994). Thus, drebrin in the supernatant could represent free drebrin and those loosely attached to the plasma membrane. This interpretation agrees well with the SIG labeling PATTERN, which showed membranous labeling for drebrin A more at PNd7 than in adulthood. The drebrin appearing in the supernatant may be the correlate of ultrastructurally observed junctional and nonjunctional drebrin at flat portions and shallow protrusions (protospines) along intracellular surfaces of dendritic membranes.

The extraction experiment shows that drebrin's association with the pellet is ionic and nonmembranous. The best candidate for an element contained within pellets

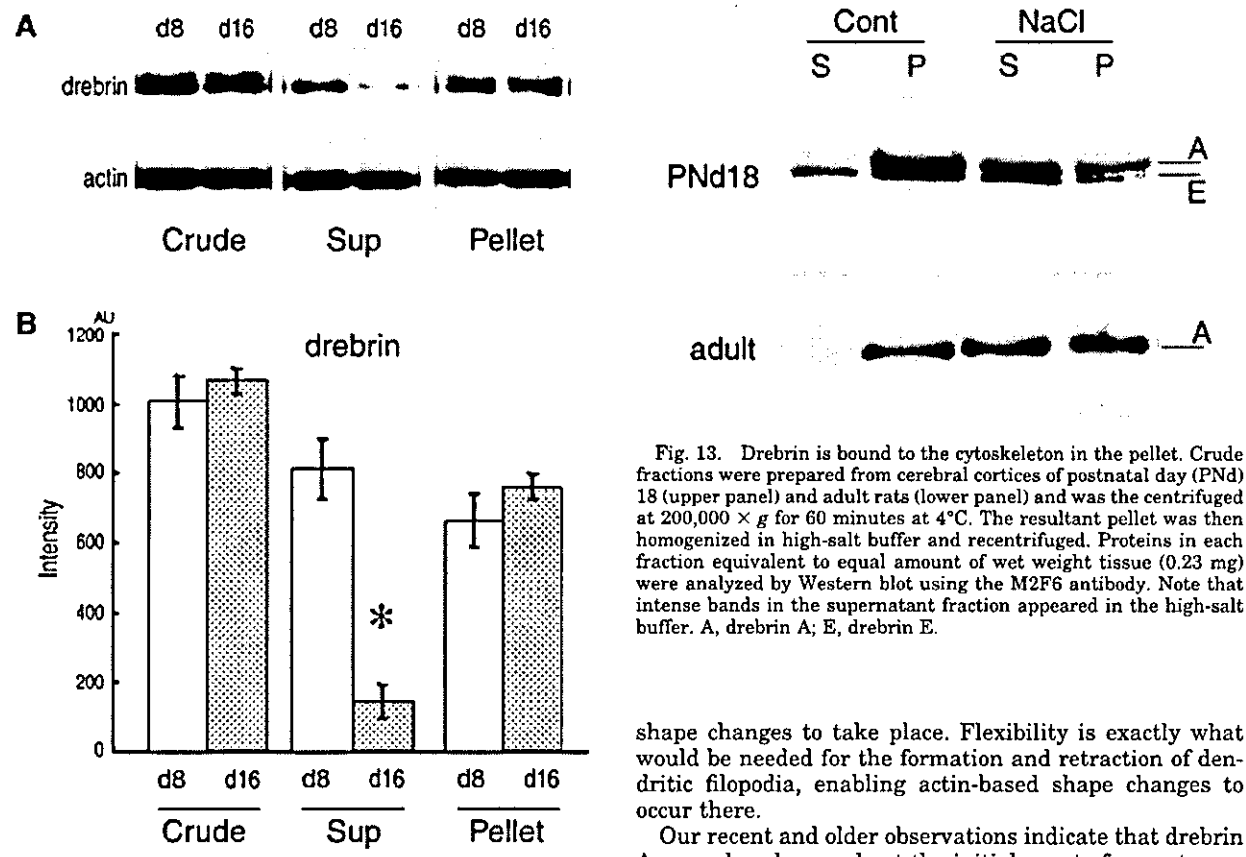

Fig. 12. Densitometric analysis of drebrin in each subcellular fraction. Each fraction equivalent to 0.23 mg of wet weight tissue was quantitatively analyzed in Western blots for drebrin content. Drebrin content was measured as intensity in Western blots from the crude, supernatant, and pellet fractions of postnatal day (PNd) 8 and PNd16 cortex homogenates. Panel A shows an example of a Western blot using M2F6 monoclonal antibody directed against drebrin and β-actin immunostaining used for comparison. Drebrin intensity in the supernatant fraction at PNd16 (d16) was significantly less than that at PNd8 (d8, n = 4, $*P < 0.001$, t test). Drebrin intensity in the crude and pellet fractions did not change during the same developmental period (n = 4; $P = 0.42$ for crude fraction; n = 4; $P = 0.30$ for the pellet fraction). AU, Arbitrary unit. Error bars indicate SEM. Histograms show mean values ± SEM.

Fig. 13. Drebrin is bound to the cytoskeleton in the pellet. Crude fractions were prepared from cerebral cortices of postnatal day (PNd) 18 (upper panel) and adult rats (lower panel) and was the centrifuged at 200,000 × g for 60 minutes at 4°C. The resultant pellet was then homogenized in high-salt buffer and recentrifuged. Proteins in each fraction equivalent to equal amount of wet weight tissue (0.23 mg) were analyzed by Western blot using the M2F6 antibody. Note that intense bands in the supernatant fraction appeared in the high-salt buffer. A, drebrin A; E, drebrin E.

that can provide ionic and nonmembranous association is the cytoskeletal matrix (Glenney et al., 1982; Yamashiro-Matsumura and Matsumura, 1985), of which F-actin is the main constituent within mature spines (Matus, 2000). Drebrin associated with F-actin in the pellet may be the component involved in the formation of spines from the shallow protrusions (protospines).

How does drebrin A associated with F-actin promote spine formation? In vitro assays have shown that drebrin reduces the association of F-actin with α-actinin and tropomyosin, possibly by binding competitively to these latter proteins' binding sites to actin (Shirao and Sekino, 2001). Because α-actinin mediates cross-linking and bundling of actin filaments, the consequence of drebrin binding to F-actin within the submembranous zone would be to relax the actin cytoskeletal matrix, thereby allowing for shape changes to take place. Flexibility is exactly what would be needed for the formation and retraction of dendritic filopodia, enabling actin-based shape changes to occur there.

Our recent and older observations indicate that drebrin A may also play a role at the initial event of synaptogenesis, that is, contact between an axon and a dendrite, even before it plays a role in spine formation. The new observation supporting this idea is that drebrin A immunoreactivity could be found along the flat submembranous surfaces of dendrites and at protospines. This finding is corroborated by earlier studies analyzing the role of drebrin upon intercellular adhesion of cells grown in culture. Specifically, Ikeda et al. (1996) observed that drebrin A transfection of fibroblasts led to the stabilization of adhesion plaques. The isoform drebrin E has been observed to interact with connexin at sites of functional GAP junctions within brain tissue (Butkevich et al., 2004) and also to occur at junctional plaques, defining a specific microfilament anchorage system in polar epithelial cells (Peitsch et al., 1999). There is additional evidence indicating that drebrin A may recruit synaptic proteins resident in spines. Interactions between PSDs and the postsynaptic cytoskeleton involve Shank, a scaffold protein (Naisbitt et al., 1999). Shank is reported to promote the maturation of dendritic spines by regulating the accumulation of spine-resident proteins, such as PSD-95, F-actin, and the NR1 subunit of NMDA receptors (Sala et al., 2001). This influence of Shank upon spine maturation, in turn, is dependent on its binding to Homer. We have shown that drebrin A, like Shank, promotes the accumulation of PSD-95 (Takahashi et al., 2003). Because Homer binds to drebrin A (Mizutani et al., 1999) as well as to Shank, drebrin A may facilitate the synaptic recruitment of Homer and Shank and, hence, the accumulation of PSD-95 and receptors for a coordinated maturation of spines and synapses.

Possible role of drebrin A in adulthood

The developmental increase of drebrin A's association with the pellet fraction and, thus, with actin indicates that drebrin A may continue to regulate dendritic shape in adulthood. Recent studies have permitted direct visualization of spines in vivo over a period of days. Such studies have shown that, indeed, spines undergo turnover throughout adulthood, with approximately 20% of those in the adult cortex disappearing within a day (Trachtenberg et al., 2002; Majewska and Sur, 2003). Spinogenesis is even more active in the hippocampus, with profound changes in spine density occurring every 4–5 days, in synchrony with the estrous cycle (Gould et al., 1990; Woolley et al., 1990; Leranth et al., 2004). The same studies and many others (Bonhoeffer and Yuste, 2002; Star et al., 2002; Konur and Yuste, 2004) have also shown that spine motility is dependent on synaptic activity (reviewed by Harris, 1999). Studies are planned that will examine the impact of overexpression and loss of expression of drebrin A and/or drebrin E upon spine and synapse formation.

ACKNOWLEDGMENTS

We thank Dr. Robert Levy for critical reading of the article and for helpful discussions.

LITERATURE CITED

Aoki C. 1997. Postnatal changes in the laminar and subcellular distribution of NMDA-R1 subunits in the cat visual cortex as revealed by immuno-electron microscopy. Brain Res Dev Brain Res 98:41–59.

Aoki C, Venkatesan C, Go CG, Mong JA, Dawson TM. 1994. Cellular and subcellular localization of NMDA-R1 subunit immunoreactivity in the visual cortex of adult and neonatal rats. J Neurosci 14:5202–5222.

Aoki C, Rodrigues S, Kurose H. 2000. Use of electron microscopy in the detection of adrenergic receptors. Methods Mol Biol 126:535–563.

Aoki C, Miko I, Oviedo H, Mikeladze-Dvali T, Alexandre L, Sweeney N, Bredt DS. 2001. Electron microscopic immunocytochemical detection of PSD-95, PSD-93, SAP-102, and SAP-97 at postsynaptic, presynaptic, and nonsynaptic sites of adult and neonatal rat visual cortex. Synapse 40:239–257.

Asada H, Uyemura K, Shirao T. 1994. Actin-binding protein, drebrin, accumulates in submembranous regions in parallel with neuronal differentiation. J Neurosci Res 38:149–159.

Bonhoeffer T, Yuste R. 2002. Spine motility. Phenomenology, mechanisms, and function. Neuron 35:1019–1027.

Butkevich E, Hulsmann S, Wenzel D, Shirao T, Duden R, Majoul I. 2004. Drebrin is a novel connexin-43 binding partner that links gap junctions to the submembrane cytoskeleton. Curr Biol 14:650–658.

Crosbie R, Adams S, Chalovich JM, Reisler E. 1991. The interaction of caldesmon with the COOH terminus of actin. J Biol Chem 266:20001–20006.

Descarries L. 1991. Non junctional relationships of monoamine axon terminals in the cerebral cortex of adult rat. Volume transmission in the brain: novel mechanisms for neural transmission. Adv Neurosci 1:53–62.

Erisir A, Levey AI, Aoki C. 2001. Muscarinic receptor M(2) in cat visual cortex: laminar distribution, relationship to gamma-aminobutyric acidergic neurons, and effect of cingulate lesions. J Comp Neurol 441:168–185.

Farb CR, Aoki C, Ledoux JE. 1995. Differential localization of NMDA and AMPA receptor subunits in the lateral and basal nuclei of the amygdala: a light and electron microscopic study. J Comp Neurol 362:86–108.

Fox JE. 1985. Identification of actin-binding protein as the protein linking the membrane skeleton to glycoproteins on platelet plasma membranes. J Biol Chem 260:11970–11977.

Fritschy JM, Brunig I. 2003. Formation and plasticity of GABAergic synapses: physiological mechanisms and pathophysiological implications. Pharmacol Ther 98:299–323.

Fujisawa S, Aoki C. 2003. In vivo blockade of N-methyl-D-aspartate receptors induces rapid trafficking of NR2B subunits away from synapses and out of spines and terminals in adult cortex. Neuroscience 121:51–63.

Glenney JR Jr, Glenney P, Weber K. 1982. F-actin-binding and cross-linking properties of porcine brain fodrin, a spectrin-related molecule. J Biol Chem 257:9781–9787.

Gould E, Woolley CS, Frankfurt M, McEwen BS. 1990. Gonadal steroids regulate dendritic spine density in hippocampal pyramidal cells in adulthood. J Neurosci 10:1286–1291.

Harris KM. 1999. Structure, development, and plasticity of dendritic spines. Curr Opin Neurobiol 9:343–348.

Hayashi K, Shirao T. 1999. Change in the shape of dendritic spines caused by overexpression of drebrin in cultured cortical neurons. J Neurosci 19:3918–3925.

Hayashi K, Ishikawa R, Ye LH, He XL, Takata K, Kohama K, Shirao T. 1996. Modulatory role of drebrin on the cytoskeleton within dendritic spines in the rat cerebral cortex. J Neurosci 16:7161–7170.

Hayashi K, Suzuki K, Shirao T. 1998. Rapid conversion of drebrin isoforms during synapse formation in primary culture of cortical neurons. Brain Res Dev Brain Res 111:137–141.

He Y, Janssen WG, Morrison JH. 1998. Synaptic coexistence of AMPA and NMDA receptors in the rat hippocampus: a postembedding immunogold study. J Neurosci Res 54:444–449.

Ikeda K, Shirao T, Toda M, Asada H, Toya S, Uyemura K. 1995. Effect of a neuron-specific actin-binding protein, drebrin A, on cell-substratum adhesion. Neurosci Lett 194:197–200.

Ikeda K, Kaub PA, Asada H, Uyemura K, Toya S, Shirao T. 1996. Stabilization of adhesion plaques by the expression of drebrin A in fibroblasts. Brain Res Dev Brain Res 91:227–236.

Imamura K, Shirao T, Mori K, Obata K. 1992. Changes of drebrin expression in the visual cortex of the cat during development. Neurosci Res 13:33–41.

Ishikawa R, Hayashi K, Shirao T, Xue Y, Takagi T, Sasaki Y, Kohama K. 1994. Drebrin, a development-associated brain protein from rat embryo, causes the dissociation of tropomyosin from actin filaments. J Biol Chem 269:29928–29933.

Jontes JD, Buchanan J, Smith SJ. 2000. Growth cone and dendrite dynamics in zebrafish embryos: early events in synaptogenesis imaged in vivo. Nat Neurosci 3:231–237.

Kojima N, Shirao T, Obata K. 1993. Molecular cloning of a developmentally regulated brain protein, chicken drebrin A and its expression by alternative splicing of the drebrin gene. Brain Res Mol Brain Res 19:101–114.

Konur S, Yuste R. 2004. Developmental regulation of spine and filopodial motility in primary visual cortex: reduced effects of activity and sensory deprivation. J Neurobiol 59:236–246.

Lendvai B, Stern EA, Chen B, Svoboda K. 2000. Experience-dependent plasticity of dendritic spines in the developing rat barrel cortex in vivo. Nature 404:876–881.

Leranth C, Hajszan T, MacLusky NJ. 2004. Androgens increase spine synapse density in the CA1 hippocampal subfield of ovariectomized female rats. J Neurosci 24:495–499.

Levy RB, Aoki C. 2002. Alpha7 nicotinic acetylcholine receptors occur at postsynaptic densities of AMPA receptor-positive and -negative excitatory synapses in rat sensory cortex. J Neurosci 22:5001–5015.

Majewska A, Sur M. 2003. Motility of dendritic spines in visual cortex in vivo: changes during the critical period and effects of visual deprivation. Proc Natl Acad Sci U S A 100:16024–16029.

Marty S, Wehrle R, Alvarez-Leefmans FJ, Gasnier B, Sotelo C. 2002. Postnatal maturation of Na+, K+, 2Cl- cotransporter expression and inhibitory synaptogenesis in the rat hippocampus: an immunocytochemical analysis. Eur J Neurosci 15:233–245.

Matus A. 2000. Actin-based plasticity in dendritic spines. Science 290:754–758.

Megias M, Emri Z, Freund TF, Gulyas AI. 2001. Total number and distribution of inhibitory and excitatory synapses on hippocampal CA1 pyramidal cells. Neuroscience 102:527–540.

Minelli A, Alonso-Nanclares L, Edwards RH, DeFelipe J, Conti F. 2003. Postnatal development of the vesicular GABA transporter in rat cerebral cortex. Neuroscience 117:337–346.

Mizutani A, Shiraishi Y, Mikoshiba K, Furuichi T. 1999. Characterization of Cupidin-binding proteins. Soc Neurosci Abst 25:805.807.

Naisbitt S, Kim E, Tu JC, Xiao B, Sala C, Valtschanoff J, Weinberg RJ, Worley PF, Sheng M. 1999. Shank, a novel family of postsynaptic

density proteins that binds to the NMDA receptor/PSD-95/GKAP complex and cortactin. Neuron 23:569–582.

Peitsch WK, Grund C, Kuhn C, Schnolzer M, Spring H, Schmelz M, Franke WW. 1999. Drebrin is a widespread actin-associating protein enriched at junctional plaques, defining a specific microfilament anchorage system in polar epithelial cells. Eur J Cell Biol 78:767–778.

Peters A. 2002. Examining neocortical circuits: some background and facts. J Neurocytol 31:183–193.

Petralia RS, Wenthold RJ. 1992. Light and electron immunocytochemical localization of AMPA-selective glutamate receptors in the rat brain. J Comp Neurol 318:329–354.

Phend KD, Rustioni A, Weinberg RJ. 1995. An osmium-free method of Epon embedment that preserves both ultrastructure and antigenicity for post-embedding immunocytochemistry. J Histochem Cytochem 43: 283–292.

Purpura DP, Pappas GD. 1972. Structure and function of synapses. New York: Raven Press.

Sala C, Piech V, Wilson NR, Passafaro M, Liu G, Sheng M. 2001. Regulation of dendritic spine morphology and synaptic function by Shank and Homer. Neuron 31:115–130.

Shirao T. 1995. The roles of microfilament-associated proteins, drebrins, in brain morphogenesis: a review. J Biochem (Tokyo) 117:231–236.

Shirao T, Sekino Y. 2001. Clustering and anchoring mechanisms of molecular constituents of postsynaptic scaffolds in dendritic spines. Neurosci Res 40:1–7.

Shirao T, Obata K. 1986. Immunochemical homology of 3 developmentally regulated brain proteins and their developmental change in neuronal distribution. Dev Brain Res 29:233–244.

Shirao T, Inoue HK, Kano Y, Obata K. 1987. Localization of a developmentally regulated neuron-specific protein S54 in dendrites as revealed by immunoelectron microscopy. Brain Res 413:374–378.

Shirao T, Kojima N, Kato Y, Obata K. 1988. Molecular cloning of a cDNA for the developmentally regulated brain protein, drebrin. Brain Res 464:71–74.

Shirao T, Kojima N, Nabeta Y, Obata K. 1989. Two forms of drebrins, developmentally regulated brain proteins, in rat. Proc Jpn Acad 65: 169–172.

Shirao T, Kojima N, Obata K. 1992. Cloning of drebrin A and induction of neurite-like processes in drebrin-transfected cells. Neuroreport 3:109–112.

Shirao T, Hayashi K, Ishikawa R, Isa K, Asada H, Ikeda K, Uyemura K. 1994. Formation of thick, curving bundles of actin by drebrin A expressed in fibroblasts. Exp Cell Res 215:145–153.

Star EN, Kwiatkowski DJ, Murthy VN. 2002. Rapid turnover of actin in dendritic spines and its regulation by activity. Nat Neurosci 5:239–246.

Takahashi H, Sekino Y, Tanaka S, Mizui T, Kishi S, Shirao T. 2003. Drebrin-dependent actin clustering in dendritic filopodia governs synaptic targeting of postsynaptic density-95 and dendritic spine morphogenesis. J Neurosci 23:6586–6595.

Trachtenberg JT, Chen BE, Knott GW, Feng G, Sanes JR, Welker E, Svoboda K. 2002. Long-term in vivo imaging of experience-dependent synaptic plasticity in adult cortex. Nature 420:788–794.

Vaughn JE. 1989. Fine structure of synaptogenesis in the vertebrate central nervous system. Synapse 3:255–285.

Woolley CS, Gould E, Frankfurt M, McEwen BS. 1990. Naturally occurring fluctuation in dendritic spine density on adult hippocampal pyramidal neurons. J Neurosci 10:4035–4039.

Yamashiro-Matsumura S, Matsumura F. 1985. Purification and characterization of an F-actin-bundling 55-kilodalton protein from HeLa cells. J Biol Chem 260:5087–5097.

Available online at www.sciencedirect.com
SCIENCE DIRECT®
Neuroscience Research 49 (2004) 205–217
Neuroscience Research
www.elsevier.com/locate/neures

Antisense knockdown of drebrin A, a dendritic spine protein, causes stronger preference, impaired pre-pulse inhibition, and an increased sensitivity to psychostimulant

Rika Kobayashi[a], Yuko Sekino[b], Tomoaki Shirao[b], Satoshi Tanaka[b], Taichi Ogura[a], Ken Inada[c], Makoto Saji[a,d,*]

[a] *Division of Brain Science, Kitasato University Graduate School of Medical Sciences, Sagamihara 228-8555, Japan*
[b] *Department of Neurobiology and Behavior, Gunma University School of Medicine, Maebashi 371-8511, Japan*
[c] *Department of Psychiatry, Kitasato University School of Medicine, Sagamihara 288-8555, Japan*
[d] *Department of Physiology, Kitasato University School of Allied Health Sciences, Sagamihara 288-8555, Japan*

Received 7 January 2004; accepted 25 February 2004

Available online 24 April 2004

Abstract

Drebrin located in dendritic spines regulates their morphological changes and plays a role in the synaptic plasticity via spine function. Reduced drebrin has been found in the brain of patients with Alzheimer's disease or Down's syndrome. To examine whether the down-regulation of drebrin protein levels causes deficits in higher brain function, such as memory or cognition, we performed antisense-induced knockdown of drebrin A expression in rat brain using an hemagglutinating virus of Japan (HVJ)-liposome gene transfer technique. We investigated the effects of drebrin in vivo knockdown on spatial memory in a water-maze task, sensorimotor gating in a pre-pulse-inhibition test, adaptive behaviors in an open-field test, and sensitivity to psychostimulant in an amphetamine-induced locomotor response. Rats with drebrin A in vivo knockdown displayed a stronger preference for a previous event due to perseverative behavior, impaired pre-pulse inhibition (PPI), increased locomotor activity, anxiety-like behavior, and an increased sensitivity to psychostimulant, suggesting behaviors related to schizophrenia. These findings indicated that decreased drebrin produces deficits in cognitive function but not in spatial memory, probably via hypofunction of dendritic spines.

Keywords: Actin-binding protein; Antisense oligodeoxynucleotides; HVJ-liposome-mediated gene transfer; Water-maze task; Locomotor activity; Cognitive function

1. Introduction

Many types of neurons have dendrites with small protrusions termed spines. In the cerebral cortex, about 75% of neurons have dendrites with a high density of spines, and most of these spiny neurons are excitatory (Keller, 2002). Furthermore, most of the excitatory synapses in the cortex make contact with the dendritic spines of other excitatory neurons (Marrs et al., 2001; Okabe et al., 2001). Since dendritic spines are specialized compartments that serve as the structural base for synaptic signaling, integration, and plasticity in mature brain, the ability of spines to alter their shape or length and the stability of synaptic contacts at spines provide a powerful mechanism for synaptic plasticity in the excitatory circuitry in the cerebral cortex and the limbic regions, such as the hippocampus and the amygdala (Engert and Bonhoeffer, 1999; Lendvai et al., 2000; Shirao and Sekino, 2001).

Drebrin A, an actin-binding protein, accumulates specifically in the dendritic spines (Hayashi et al., 1996; Shirao et al., 1987; Shirao, 1995). In recent in vitro studies, it has been demonstrated that drebrin A regulates changes in the shape and density of dendritic spines, probably via the rearrangement of cytoskeletal actin filaments (Hayashi and Shirao, 1999; Shirao et al., 1994). In particular, high expression of drebrin A is specifically observed in the cerebral cortex, hippocampus, amygdala, thalamus, and striatum (Hayashi et al., 1996; Shirao and Obata, 1986), which are responsible

* Corresponding author. Tel.: +81-427-78-8311; fax: +81-427-78-8153.
E-mail address: sajim@ahs.kitasato-u.ac.jp (M. Saji).

0168-0102/$ – see front matter © 2004 Elsevier Ireland Ltd and The Japan Neuroscience Society. All rights reserved.
doi:10.1016/j.neures.2004.02.014

for higher brain functions. Clinically, a marked decrease of drebrin A was found in brains with Alzheimer's disease (Harigaya et al., 1996; Hatanpaa et al., 1999) or Down's syndrome (Shim and Lubec, 2002). The synaptic plasticity of the excitatory circuitry underlying higher brain functions, such as learning, memory, or cognition is considered to involve a stimulus-dependent change of the shape and density of dendritic spines (Keller, 2002; Marrs et al., 2001; Okabe et al., 2001; Shirao and Sekino, 2001). Therefore, it is hypothesized that experimentally induced knockdown of drebrin A, dendritic spine protein, in the whole brain could cause some defects in memory formation, sensorimotor gating function, or cognitive function.

To examine whether the dysfunction or hypofunction of dendritic spine-mediated synaptic function in the excitatory circuitry in the forebrain causes defects in spatial reference memory, adaptive response to a novel environment, and sensorimotor gating, we performed antisense-induced down-regulation of drebrin A expression in the forebrain regions. In rats with long-lasting knockdown of drebrin A expression in the forebrain regions, such as the neocortex or hippocampus, we tested spatial learning using the Morris water-maze task, an adaptive response to a novel environment in an open-field test, psychostimulant sensitivity using an amphetamine-induced locomotor response, and sensorimotor gating function in the pre-pulse inhibition (PPI) test of the acoustic startle response, all of which are sensitive to anti-glutaminergic drugs and lesions of the hippocampus (Bakshi and Geyer, 1998; Carlsson and Carlsson, 1990; Ellison, 1995; Morris et al., 1982). To achieve a long-lasting in vivo knockdown of drebrin A expression by a single intra-ventricular injection of antisense oligodeoxynucleotides (ODNs), we chose to use a combination of the antisense technique and the hemagglutinating virus of Japan (HVJ)-liposome-mediated gene transfer method. HVJ-liposome-mediated gene transfer is a method that enables delivery of the contents (ODNs) of the HVJ-liposome vector directly into cells by means of the Sendai virus (HVJ)-cell fusion machinery (Inada et al., 2003; Iwakuma et al., 2003; Kobayashi et al., 2002; Saeki et al., 1997; Yamada et al., 1996). Down-regulation of drebrin A by the antisense ODNs we used in the present study has induced the attenuation of synaptic clustering of PSD-95 as well as clustering of drebrin and F-actin in cultured hippocampal neurons (Takahashi et al., 2003).

2. Materials and methods

2.1. Animal care

Ninety six naïve, 10-week-old, male Wistar rats weighing 230–280 g (Japan SLC, Kanagawa, Japan) were used in the present study. The animals were housed in clear plastic cages in groups of two or three and were allowed access to food and water throughout the experiment. The animals were maintained in a temperature-, humidity-, and light-controlled environment with a 12 h light/dark cycle. On arrival in the colony, the experimenter holds the animal gently by the body rubbing its head and back for about 5 min. Not to be in fear of the experimenter, this type of handling was performed once a day for several days or a week until the surgical operation for the intra-ventricular injection of HVJ-liposomes containing ODNs was conducted.

All experiments conformed to Japanese and international guidelines on the ethical use of animals, and every effort was made to minimize the number of animals and their suffering.

2.2. Oligodeoxynucleotides (ODNs)

Phosphotioated ODNs (24 mers) corresponding to a specific segment in the 5′-coding region of drebrin cDNA were designed to selectively deacrese byosynthesis of the drebrin A as antisense ODNs to drebrin A (Dre-AS: 5′-AGGA-AGGCCCACTGTCCGATGCCT-3′)(Takahashi et al., 2003; Tanaka et al., 2001). Reversed antisense ODNs (Dre-RE: 5′-TCCGTAGCCTGTCACCCGGAAGGA-3′), in which the bases of the 24 mers corresponding to Dre-AS were reversed, were synthesized for use as a control. A search of the Genebank/EMBL database determined that none of the ODN sequence overlapped with other mammalian sequences.

2.3. Preparation of HVJ-liposome containing ODNs

The detailed preparation of anionic HVJ-liposome containing ODNs has been described elsewhere (Iwakuma et al., 2003; Saeki et al., 1997; Yamada et al., 1996). Briefly, three kinds of lipids (phosphatidylserine, phosphatidylcholine, and cholesterol) dissolved in chloroform (1 mg/ml) were mixed in a weight ratio of 1:4.8:2. One milligram of the lipid mixture was transferred into a glass tube and dried as a thin lipid film using a rotary evaporator filled with nitrogen gas at 40 °C. The lipid thin film layering on the bottom of a glass tube was hydrated in 200 μl of a balanced salt solution (BSS: 137 mM NaCl, 5.4 mM KCl, 10 mM Tris–HCl, pH 7.5) containing 100 μg of ODNs which were dispersed in the aqueous phase at room temperature. The mixture of the hydrated lipid thin film and ODNs was agitated by vortexing for 30 s and then incubated at 37 °C for 30 s. This procedure was repeated eight times, making fragments of lipid thin film into liposomes in which ODNs were packaged up. The liposome suspension was sonicated for 20 s and vortexed for 30 s. Then 300 μl of BSS was added to the liposomes suspension and incubated at 37 °C for 30 min shaking. The liposome suspension prepared above (500 μl) was mixed with 1 ml HVJ suspension (more than 10,000 hemagglutinating units), whose RNA genome had been inactivated by ultraviolet irradiation (198 mJ/cm^2) just before use. The mixture was incubated at 4 °C for 10 min and at 37 °C for 1 h shaking to facilitate the fusion between the inactivated HVJ and the liposomes. The ODNs–HVJ–liposome complex was loaded onto a discontinuous sucrose gradient and

centrifuged at 25,000 rpm at 4 °C for 1.5 h to separate the ODNs–HVJ–liposome complex from free HVJ. The purified ODNs–HVJ–liposomes suspension was adjusted to OD 1.0 (540 nm) with 200–250 μl of BSS. Since 10–30% of ODNs (10–30 μg) are available for packing into the liposomes (Kaneda, 1999), it is estimated that 1 μl of the purified ODNs–HVJ–liposomes (OD 1.0) contains about 40–120 ng of ODNs.

2.4. Intra-ventricular injection of an HVJ-liposome vector containing ODNs

Rats were anesthetized with an intra-peritoneal injection of pentobarbital sodium (40 mg/kg). A total of 30 μl (1.2–3.6 μg ODNs) of HVJ-liposome vectors containing ODNs was stereotaxically injected into both sides of the lateral ventricle in the rats. The coordinates for intra-ventricular injection in mm in respect to ear bar were; (1) AP: 8.2; L: +1.4; D: 3.8 and (2) AP: 8.2; L: −1.4; D: 3.8. A glass micropipette (tip size: 30–40 μm; volume: 2.5 μl/mm) made from a disposable micropipette (20 μl, Drummond), which was connected to an air pressure system with polyethylene tubing, was used for a single intra-ventricular injection of the HVJ-liposome vectors containing ODNs (Iwakuma et al., 2003).

2.5. Western blot analysis

For quantification of the protein expression levels, Western blot analysis was used. Rats were anesthetized with diethyl ether and decapitated at various days after the intra-ventricular injection of HVJ-liposome vectors containing antisense ODNs or reversed antisense ODNs. The hippocampus, neocortex, cerebellum and thalamus were quickly dissected out of the removed brain and stored at −80 °C before use. The tissue (100 μg per 1 μl buffer) was sonicated in cold sample buffer containing 40% glycerol, 20% Tris-glycine, 2% sodium dodecylsulfate (SDS), 5% 2-mercaptoethanol until the homogenate was uniform. The homogenate was centrifuged at 15,000 rpm for 10 min at 4 °C and denatured for 3 min. The supernatant of 4 μl was loaded on 8% sodium dodecylsulfate–polyacrylamide gel (40 μg protein per lane) and separated by electrophoresis. Separated proteins were transferred electrophoretically from the gel to a polyvinylidine difluoride (PVDF) membrane (ATTO, Tokyo, Japan). After being blocked with blocking buffer (Block Ace, Dainihon Seiyaku, Japan) at 4 °C for 1 h for drebrin A or overnight for β-actin, the membrane was processed with the primary antibodies overnight at room temperature for more than 1 h. Two primary antibodies were used, a rabbit polyclonal antibody against drebrin A (1:1000, produced by Dr. T Shirao) (Shirao et al., 1994) and a monoclonal antibody against β-actin (1:3000, Abcom, UK). After being washed in PBS containing 0.1% Tween for 1 h, the membrane was incubated with the second antibody, peroxidase-conjugated goat anti-rabbit IgG (1:2000 for drebrin A, 1:10000 for β-actin, Leinco Technologies) at room temperature for 1 h. Then the membrane was processed with enhanced chemiluminescence reagents to visualize the antibody reaction using an ECL detection kit (Amersham International, UK) and finally exposed to X-ray film (Kodak). Western blots were analyzed with computer densitometory by using NIH image software for quantification of drebrin A protein levels. For the measurement of β-actin as control protein, the membrane was reprobed with monoclonal antibody against β-actin to confirm equal protein loading in each lane. The mean optical densities of bands for two samples per animal were determined, and the film background was subtracted. The band densities for drebrin A or β-actin protein in treated rats were represented as relative percentages of those in non-treated control rats. The mean band densities thus obtained were statistically analyzed with one-way ANOVA and post-hoc Fisher's test to determine the significance.

2.6. Open field test for spontaneous locomotor activity, adaptive behaviors and amphetamine-induced locomotor response

A rat was placed in the center of a white square box (width, 1.0 m; height, 0.4 m). The locomotor behavior of the rat was recorded by a video camera during the initial 30 min period following the start of spontaneous locomotion in the open field. In experiment for psychostimulant-sensitivity, the locomotor behavior of the rat was recorded during the total 90 min period that consists of the initial 30 min period (pre-injection) after the start of spontaneous locomotion and the following 60 min period (post-injection) of amphetamine-induced locomotor response by the intra-peritoneal administration of amphetamine (1.0 mg/kg). From the 30 min or 90 min recording of locomotor behavior, rat position was tracked by computer and the locomotor distance during every 5 min period was measured as a locomotor activity using computer-guided image software (Kurihara Medical Instrument, Tokyo).

As for typical behaviors in adaptive response to a novel environment, a total duration of being stationary, being exploratory or grooming during the 30 min test period was measured from the 30 min recording of behaviors following the start of spontaneous locomotion in an open field, respectively. Being exploratory means both horizontal locomotion and vertical locomotion including rearing, while being stationary is defined as a stationary state without grooming or rearing.

2.7. Prepulse inhibition test of acoustic startle response

A startle chamber with a floor equipped with an electric weighing machine and a speaker mounted 24 cm above the floor for presenting acoustic noise burst was used. Rats were placed in the startle chamber and allowed to acclimate for 5 min before the test session. Background noise

was set at 65 dB of white noise throughout the acclimation period and test session. In a test session, 10 trials of three types of acoustic stimulation (total 30 trials) were given in pseudo-random order after initial startle-stimuli (20 ms burst of 120 dB). One of the three types was a startle pulse alone (P alone) trail, which involved a 20 ms burst of 120 dB, and the other two types were a combined trial of prepulse and startle pulse (PP70 &P and PP80 &P), which involved a 20 ms burst of 70 dB or 80 dB as a prepulse, respectively, followed by the same pulse as in the P alone trial 100 ms later. The inter-trial intervals averaged 40 s (20–60 s) were given in pseudo-random order. In addition to these three types of trials, no-stimulus (non-stim) trials were inserted between trials to check the baseline amplitude without stimulation. The startle response was measured for 100 ms from the startle pulse presentation, and the average value was defined as the startle amplitude. The startle amplitudes in response to repetitions of each trial type were averaged over the session. The test schedule was controlled by a microcomputer.

The percent prepulse inhibition (% PPI) of a startle response was calculated by the following formula:

$$\%\text{PPI at PP80} = \left\{1 - \frac{\text{PP80 \&P}}{\text{P alone}}\right\} \times 100$$

$$\%\text{PPI at PP70} = \left\{1 - \frac{\text{PP70 \&P}}{\text{P alone}}\right\} \times 100$$

2.8. Water-maze task training for spatial reference memory

We used the Morris water-maze task to test for an acquisition of spatial reference memory. The apparatus used for the hidden platform task in water-maze consisted of a white circular pool (diameter, 1.5 m; height, 0.5 m) filled to a depth of 20 cm with clear water (24±2 °C) and a transparent plastic platform (diameter, 15 cm; height, 0.3 m) submerged 2 cm below the water surface. Rats were given 6 consecutive training trials (a session) per day with an inter-trial interval of 60 s, from random starting location, with a hidden platform in a fixed position. Training sessions were performed over 5 consecutive days (total 30 trials). For each trial, rats had a maximum of 60 s swim time to mount the platform and they were then allowed to rest on the platform for additional 15 s. Rats were placed on the platform for 15 s manually if they elapsed. Rat position was tracked by computer, and the swim time was measured as the escape latency some rats that stayed longer making circle along the periphery of the pool in the session 1 were eliminated from the further training sessions.

On the last day of training session, a spatial probe test was conducted 60 s after the end of the last training session. Rats were given a 60 s-probe trial in which the hidden platform had been removed from the pool. For each probe test rat position was tracked by computer and the time spent in each quadrant zone was measured as the place preference. Each quadrant zone was defined as follows: target, the quadrant in which the hidden platform had been positioned; opposite, the quadrant opposite to the target; right, the quadrant on the right side of the target; left, the quadrant on the left side of the target.

2.9. Statistics

All statistical analysis was carried out by one-way ANOVA. Post–hoc individual comparison of paired groups was carried out by using Fisher's PLSD or the Student's *t*–test. A value of $P < 0.05$ was considered to represent a significant difference.

3. Results

3.1. Antisense-induced down-regulation of drebrin A protein levels and its time course

We first used Western blot analysis with antibodies against drebrin A and β-actin to examine the regional differences in the levels of drebrin A protein expression in the forebrain and cerebellum. Fig. 1 shows representative blots and quantitation of relative band densities for drebrin A and β-actin obtained from the neocortex, cerebellum, hippocampus, and thalamus of non-treated control rats. As shown in Fig. 1, drebrin A protein expression was clearly rich in the neocortex, hippocampus, and thalamus but poor in the cerebellum, while β-actin protein levels were almost uniform in all four brain regions.

We then examined the antisense-induced change in the protein levels in the two drebrin-rich regions of the forebrain, the neocortex, and hippocampus, at 4, 8, and 18 days after the intra-ventricular injection of HVJ-liposome vectors containing Dre-AS or Dre-RE. The levels of drebrin A protein in the neocortex of the rats treated with Dre-AS decreased markedly at 4 days after injection, remained reduced for several days, and returned to the original level by 18 days post-injection, while the levels of drebrin A protein in the Dre-RE-treated rats remained unchanged at 4 days post-injection. On the other hand, in the neocortex of the Dre-AS-treated rats and Dre-RE-treated rats, the β-actin protein levels did not change at any time post-injection (Fig. 2A). As shown in the quantitative analysis for drebrin A protein levels (Fig. 2B), a significant reduction of 53.7 ± 13.2% (mean ± S.E.M., $n = 7$, 4 days post-injection) or 44.7±12.1% (mean±S.E.M., $n = 7$, 8 days post-injection) in drebrin A protein level was specifically found in the neocortex of the Dre-AS-treated rats and was sustained for more than a week, while the Dre-RE treatment did not affect the drebrin A protein levels. As shown in the quantitative analysis for β-actin protein levels (Fig. 2C), a significant change of the β-actin protein levels was not found in the neocortex of the rats treated with Dre-AS or Dre-RE at any time post-injection.

The amount of drebrin A in the hippocampus of the rats treated with Dre-AS decreased markedly at 4 days after